Viscous Dampers for Optimal Reduction in Seismic Response

Navin Prakash Verma

(ABSTRACT)

To model dissipation of energy in vibrating civil structures, existence of viscous damping is commonly assumed primarily for mathematical convenience. In such a classical damper, the damping force is assumed to depend only on the velocity of deformation. Fluid viscous dampers that provide this type of damping have been manufactured to provide supplementary damping in civil and mechanical systems to enhance their performance. Some fluid dampers, however, exhibit stiffening characteristics at higher frequencies of deformation. The force deformation relationship of such dampers can be better represented by the Maxwell model of visco-elasticity. This model consists of a viscous dashpot in series with a spring, the latter element providing the stiffening characteristics. This study is concerned with the optimal utilization of such Maxwell dampers for seismic performance improvement of civil structures.

The force deformation relationship of Maxwell dampers is described by a first order differential equation. Earlier studies dealing with these dampers, used an unsymmetric set of equations for combined structure and damper system. The solution of such equations for response analysis or for optimization calculation by a modal analysis approach would require the pair of the left and right eigenvectors. In this study, an auxiliary variable is introduced in the representation of a Maxwell damper to obtain symmetric equations of motion for combined structure and damper system. This eliminates the need for working with two sets of eigenvectors and their derivatives, required for optimal analysis.

Since the main objective of installing these dampers is to reduce the structural response in an optimal manner, the optimization problem is defined in terms of the minimization of some response-based performance indices. To calculate the optimal parameters of dampers placed at different location in the structure, Rosen's gradient projection method is employed. For numerical illustration, a 24-story shear building is considered. Numerical results are obtained for seismic input defined by a spectral density

function; however, the formulation permits direct utilization of response spectrum-based description of design earthquake. Three different performance indices -- inter story drift-based, floor acceleration-based, and base shear-based performance indices-- have been considered to calculate the numerical results. A computational scheme is presented to calculate the amount of total damping required to achieve a desired level of response reduction. The effect of ignoring the stiffening effect at higher frequencies in the Maxwell model on the optimal performance is evaluated by parametric variation of relaxation time coefficient. It is observed that the models with higher relaxation time parameter show a decreased response reducing damping effect. Thus ignoring the stiffening effect when it is, indeed, present would provide an unconservative estimation of the damping effect. The effect of brace flexibilities on different performance indices is also investigated. It is observed that flexibility in a brace reduces the effectiveness of the damper.

To My Dear Parents…

Acknowledgments

It was first time that I moved out of my town in India for so long and that too 10,000 miles away from home to pursue graduate education at Virginia Tech. But, my two years on the campus have been extremely satisfying and enjoyable. This is a good place to express few words for the people who have made my stay memorable.

I express my deep sense of gratitude to my advisor, Professor Mahendra P. Singh, for all the help not only during the course of my thesis and academics but my stay at Virginia Tech. His help, in the form of moral and technical support, affection towards me and the spirited scientific temperament towards the work was key for the completion of this work.

I would also like to express my appreciation to Dr R. C. Batra and Dr. S. L. Hendricks for kindly serving in my committee and giving their valuable time to read this manuscript.

I take this moment to thank all the people and friends I have met in Blacksburg during past two years. I have great respect for Pramod who has acted as my friend cum mentor from time to time. I express my gratitude to Sarbjeet, Prahalad, Prateep, Rajan, Prashanth, Srinivas, Jiten, Nirmala, Konda and Ravi. I will always remember the good time spent with Nishant, Deepak, Surya, Bipul, Naren, Shailesh and many others. The wonderful moments shared with them in the trips outside Blacksburg and in day-to-day life will always be cherished. I would also like to thank Luis Moreschi, who at time to time gave me his expert advice on various things related to thesis.

I dedicate my work to my dear parents who have struggled throughout life to give their children the very best. Both my parents have been supportive of my decisions and I am thankful for all their faith in me.

This research was financially supported by National Science Foundation Grant No. CMS-9987469. This support is gratefully acknowledged.

Navin Prakash Verma

Contents

List of Figures

List of Tables

Chapter 1

Introduction

1.1 Overview of Passive Structural Control

Design of structures to reduce vibrations due to external environmental forces such as winds, earthquakes etc, has been a major concern of engineers for many years. Earthquake induced ground motions often give a large amount of energy to structures and thus make them more susceptible to sudden damage. The current design practices allow the structure to yield so as to absorb this huge amount of external energy without getting collapsed. This is achieved by allowing inelastic cyclic deformations in specially detailed regions in a structure. This strategy is effective but it may render a structure irreparable. The consideration of actual dynamic nature of environmental forces has given rise to newer and innovative techniques of structural protection. The focus of research in past few years has been shifted in reducing the response of the structures due to external forces by employing special protective systems. Besides reducing damage, these methods have been successful in increasing safety of the structure.

These protective systems work on the following philosophy. The earthquake motions impart potential and kinetic energy to the structure, which makes them vibrate. A part of this energy is also absorbed by inherent damping characteristics of the structure. The protective systems either prevent the energy from reaching the structure or enhance the energy dissipation capacity. Base isolation systems are designed to prevent the energy reaching the structure by filtering it out. The energy dissipation systems on the other hand absorb the energy that reaches the structure in special devices called dampers. Several different types of energy dissipation systems have been developed. They are viscous dampers, visco-elastic dampers, friction dampers, and yielding metallic dampers. There are also tuned mass or tuned liquid dampers, which primarily store some of the structural

energy in their deformation and motion, and rely much less on energy dissipation. More complete details on the mechanics and working principles of these devices can be found in the excellent treatise by Soong and Dargush (1997) and Constantinou, Soong and Dargush (1998). The basic philosophy of passive energy control system is shown in Figure 1.1.

This study focus will focus on fluid visco-elastic dampers, and especially on those that need to be modeled by Maxwell viscoelastic damper models.

1.2 Viscoelastic Devices

The visco-elastic devices are of two types: (a) solid viscoelastic devices and, (b) fluid visco-elastic devices. The solid visco-elastic dampers consist layers of polymeric material that are allowed to deform in shear between two or more steel plates. When mounted in a structure, the structural vibration induces relative motion between the steel plates, causing shear deformation of the visco-elastic material and hence energy dissipation. For convenience of analysis, the force–deformation characteristics of these viscoelastic devices can be modeled by the Kelvin model. The fluid visco-elastic device on the other hand operates on the principle of resistance of a viscous fluid flow through a constrained opening. There are also fluid dampers that deform highly viscous fluid in shear to dissipate energy and to provide stiffness. The focus of this study is, however, only on the fluid orifice dampers. The dissipation of energy occurs via conversion of mechanical energy to thermal energy as a piston forces a viscous fluid substance through a restricted opening (Figure 1.2). The force-deformation characteristics of such devices can be designed to behave as linear viscous dampers in which forces are only proportional to the velocity of deformation (Makris *et. al.*, 1993, 1995). This is the classical form of a viscous damper that is so commonly used in analytical studies. Such dampers give rise to damping forces that are out-of-phase with deformation and deformation dependent forces. So, they do not add to maximum forces developed in structural elements. They can be very effective in reducing drifts. However, some of these fluid orifice dampers cannot be accurately modeled by the classical velocity-dependent model as they also offer resistance and provide stiffness to the system at higher frequencies of deformation. Different mathematical models have been proposed to capture their behavior in analysis.

Such dampers have been modeled by classical Maxwell model or its modified version with fractional derivatives (Makris and Constantinou, 1991). In this study, the dampers characterized by the classical Maxwell model will be used as the devices of choice for energy dissipation of structures exposed to earthquake induced ground motion. The formulation to analyze structures installed with such dampers is developed. This analytical procedure is used to select optimal design parameters of these dampers to achieve pre-selected performance objectives such as reduction of certain response quantities or minimize certain performance indices.

In the following section, we provide the organization of this study.

1.3 Thesis Organization

The thesis is organized in five chapters including Chapter 1, which gives a background and a brief overview of passive energy dissipation system.

Chapter 2 describes the models that are commonly used to characterize the viscous dampers. Equations of motion of a structure installed with viscous dampers modeled as Maxwell dampers are developed in analytically convenient form. The methodology to calculate response of structures with such equations of motions is then presented.

Chapter 3 describes the formulation of the constrained optimization problem to calculate the optimal parameters of the devices to achieve certain performance objectives in an optimal manner. The details of a gradient-based approach suitable to solve the optimization problem are provided. Numerical results are obtained to demonstrate the application of the optimization scheme.

The damping devices are attached to the building structure through braces installed in each story. These braces were considered rigid for the formulation developed in Chapter 3. In Chapter 4, the effect of the flexibility of braces on the optimal design is examined. A new optimization problem which now treats the brace stiffness as design variables in addition to the damping coefficients is formulated and solved. The effect of bracing flexibility is then evaluated through several numerical examples, presented in this chapter.

Chapter 5 presents the summary and concluding remarks about this study.

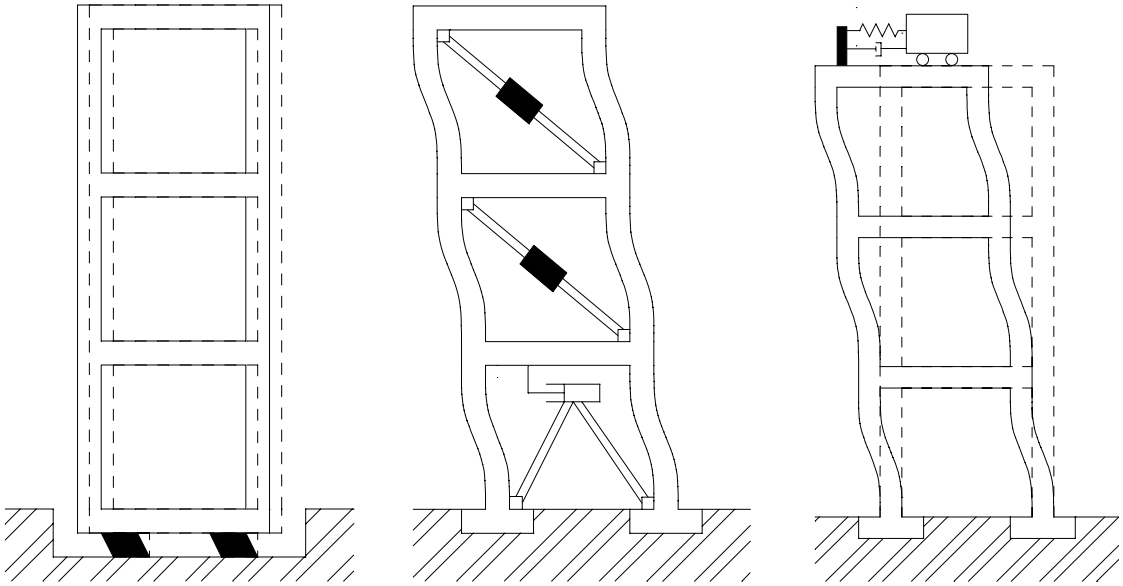

Figure 1.1: Passive response control systems, (a) seismic isolation, (b) energy dissipation devices, (c) dynamic vibration absorbers (Moreschi, 2000).

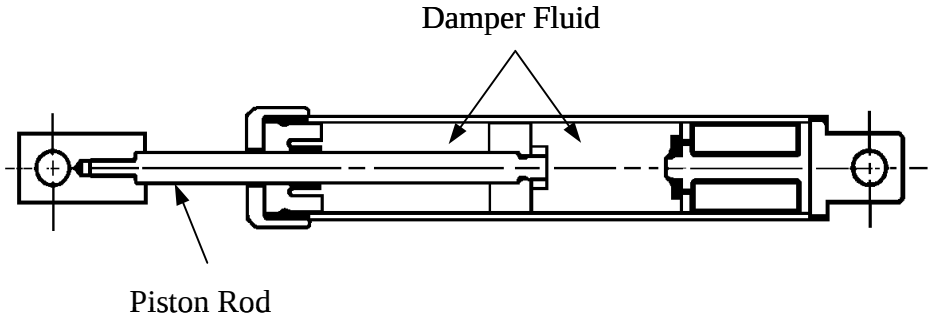

Figure 1.2: A Taylor Device Damper (Constantinou *et. al*., 1993).

Chapter 2

Analytical Formulation

2.1 Introduction

In this chapter we develop the equations of motion of structure installed with supplementary viscous damping devices. Different methods used for modeling viscous dampers are discussed in brief. Since the main focus of this work is to study the optimal design of structures with dampers described by Maxwell model, more attention is paid to develop the equations of motion with this type of model. In earlier works by Constantinou and Symans, (1993); Soong and Dargush, (1997); Moreschi (2000), non-symmetric equations were used to investigate the effect of these dampers in structures. It was, however, realized that one could also develop symmetric equations of motion, which will simplify the response analysis as well as optimal design investigation. Therefore, in Section 2.3, the symmetric equations of motion have been developed. In Section 2.4, the steps of the approach used to solve these equations of motion for earthquake inputs are described, and the necessary expressions used to calculate the response are provided. These expressions are used in the subsequent chapters and the numerical study.

2.2 Equations of Motion

Consider an *n*-degree of freedom building structure with supplementary energy dissipation devices installed at different locations. For a structure subjected to ground excitations at the base, the equations of motion can be written as:

$$\mathbf{M}_s\ddot{\mathbf{x}}(t)+\mathbf{C}_s\dot{\mathbf{x}}(t)+\mathbf{K}_s\mathbf{x}(t)+\sum_{d=1}^{n_l}\mathbf{r}_d P_d(t)=-\mathbf{M}_s\mathbf{E}\ddot{X}_g(t) \tag{2.1}$$

The system matrices involved in the equations $\mathbf{M}_s$, $\mathbf{K}_s$ and $\mathbf{C}_s$ represent, respectively, the $n \times n$ mass, structural stiffness and inherent structural damping matrices; $\ddot{X}_g(t)$ is the ground acceleration time history, $\mathbf{E}$ is the ground motion influence coefficients; $\mathbf{x}(t)$ is the *n*-dimensional relative displacement response vector measured with respect to the base. A dot over a quantity indicates time derivative of the quantity. $P_d(t)$ represents the force in the damper at the d^{th} location, and there are n_l number of possible locations where the devices can be installed on the structure. The influence of the damper force on the structure is considered through the *n*-dimensional influence vector $\mathbf{r}_d$.

In general form, the force in a damper can be described by the expression of the following form:

$$P_d[d_1, \ldots, d_n, h_d(t), \boldsymbol{\Delta}_d(t), \dot{\boldsymbol{\Delta}}_d(t), t] = 0 \tag{2.2}$$

where d_i represents the mechanical parameters related with the behavior of the devices, $h_d(t)$ is an internal variable of the device required in some models, and $\boldsymbol{\Delta}_d(t)$ is the local deformation of the d^{th} device. The local deformation of the device can be related to that of the main structure by the simple expressions as:

$$\Delta_d(t) = \mathbf{r}_d^T(t)\mathbf{x}(t) \tag{2.3}$$

2.2.1 Classical Viscous Dampers

Depending upon the characteristics of the dampers and the analytical models used, Eq. (2.2) can take different forms. The most common model often used in classical vibration studies is the linear dashpot model (Figure 2.1). In this model the damper force is assumed to be directly proportional to the damper velocity as follows:

$$P_d(t) = c_d \dot{\boldsymbol{\Delta}}_d(t) \tag{2.4}$$

In elementary vibration studies, this model is used primarily for mathematical simplification of the energy damping mechanism that is inherent in mechanical and structural systems. In Eq. (2.1), the term associated with the damping matrix is precisely based on this model. Actual dampers have also been manufactured to provide such linear velocity dependent forces.

Using the relationship Eq. (2.3) between the local deformation at a damper and the displacement vector $\mathbf{x}(t)$ into Eq. (2.4), the damper force can be expressed in terms of the structural response as follows:

$$P_d(t) = c_d \mathbf{r}_d^T(t)\dot{\mathbf{x}}(t) \tag{2.5}$$

Substituting Eq. (2.5) into Eq. (2.1), the combined equations of motion for the case of pure viscous damper can be written as

$$\mathbf{M}_s\ddot{\mathbf{x}}(t) + \left(\mathbf{C}_s + \sum_{d=1}^{n_l} \mathbf{r}_d c_d \mathbf{r}_d^T(t)\right)\dot{\mathbf{x}}(t) + \mathbf{K}_s\mathbf{x}(t) = -\mathbf{M}_s\mathbf{D}\ddot{X}_g(t) \tag{2.6}$$

The damping matrix of the system is thus modified by the installation of the dampers. This combined damping matrix of the system can be written as

$$\mathbf{C} = \mathbf{C}_s\dot{\mathbf{x}}(t) + \sum_{d=1}^{n_l} \mathbf{r}_d c_d \mathbf{r}_d^T(t) \tag{2.7}$$

It is noted that even if the initial structure is classically damped, the combined damping matrix, Eq. (2.7), of the system can become non-classically damped because of the supplementary damping terms. This means that one cannot use the undamped mode shapes to uncouple the equations of motion, but must use the state vector formulation if modal analysis is to be performed. The use of the state vector-based modal analysis approach also becomes necessary if a response spectrum analysis is to be performed.

In the state vector formulation, Eq. (2.6) can be written in the following form:

$$\mathbf{A}_s\,\dot{\mathbf{z}}(t) + \mathbf{B}_s\,\mathbf{z}(t) = -\mathbf{D}_s \begin{Bmatrix} \mathbf{0} \\ \mathbf{E} \end{Bmatrix} \ddot{X}_g(t) \tag{2.8}$$

where

$$\mathbf{A}_s = \begin{bmatrix} \mathbf{0} & \mathbf{M}_s \\ \mathbf{M}_s & \mathbf{C} \end{bmatrix}; \quad \mathbf{B}_s = \begin{bmatrix} -\mathbf{M}_s & \mathbf{0} \\ \mathbf{0} & \mathbf{K}_s \end{bmatrix}; \quad \mathbf{D}_s = \begin{bmatrix} \mathbf{0} & \mathbf{0} \\ \mathbf{0} & \mathbf{M}_s \end{bmatrix} \tag{2.9}$$

In this case, it is noted that the state matrices are symmetric. To solve these equations by a modal analysis approach, one first calculates the eigenproperties of the first order system, and then uses them to uncouple the system of equations. Since the matrices are symmetric, the left and right eigenvectors remain the same. The approach is described in several publications (Singh, 1980, Igusa *et al.*, 1984).

The classical dashpot model provides a simple approach to include the energy dissipation mechanisms inherent in the systems and devices if it is appropriate. However, previous research has shown that the classical dashpot modeling of viscoelastic devices is effective only at low frequency range of operation, and that the viscous damping devices exhibit some stiffening characteristics at high frequencies of cyclic loading. To incorporate this observed stiffening characteristics at high frequencies, a linear spring is added to the dashpot in the model. The addition of spring may be done in two ways. The spring may be attached in parallel or in series to a dashpot. The model in which the spring is added in parallel is referred to as the Kelvin model whereas the other one in which the spring is added in series is known as the Maxwell model. The analytical description and characteristics of these two models are described in the following paragraph.

2.2.2 Kelvin Damper Model

In this model, a spring is attached in parallel to the dashpot as shown in Figure 2.1. The force-displacement relations for the resulting model is given as (Zhang and Soong, 1989):

$$P_d(t) = k_d(\omega)\boldsymbol{\Delta}_d(t) + c_d(\omega)\dot{\boldsymbol{\Delta}}_d(t) \tag{2.10}$$

where k_d and c_d denote, respectively, the stiffness and damping coefficients of the model. To include the frequency dependence in this model, the coefficients have been expressed as functions of ω to render them frequency dependent. This model has been used to characterize the solid visco-elastic (VE) material in a damper. Solid VE dampers utilize copolymers or glossy substances, which dissipate energy when subjected to shear deformation. A typical VE damper consists of viscoelastic layers bonded with steel plates, which are subjected to shear deformations during vibrations. In that case, simplified expressions for the stiffness and damping coefficients in Eq. (2.13) can be written in terms of the storage and loss modulus of the material and the dimensions of the viscoelastic layers as (Zhang and Soong, 1992; Soong and Dargush, 1997)

$$k_d(\omega) = \frac{AG'(\omega)}{h}, \qquad c_d(\omega) = \frac{AG''(\omega)}{\omega h}, \tag{2.11}$$

where $G'(\omega)$ and $G''(\omega)$ are defined, respectively, as the shear storage modulus and shear loss modulus of the viscoelastic material, and ω is the frequency at which the deformation occurs, and A and h are the shear area and thickness, respectively, of the material under shear. For practical applications, the mechanical properties k_d and c_d, though dependent on the deformation frequency ω, are considered nearly constants within a narrow frequency band and operating temperature. For the analysis of structures installed with these dampers, the values of these parameters corresponding to the dominant frequency of the structure can be used to obtain useful results.

2.2.3 Maxwell Damper Model

In the Maxwell model, the spring and dashpot are placed in series. This model is schematically shown in Figure 2.2. The figure also shows the deformations of the spring and damping elements under the applied force. Let these deformations of the spring element and damper element be Δ_1 and Δ_2, respectively. The figure 2.2 also shows the free body diagrams of each element. For a given force in this damping system, the force balance equation gives,

$$k_d \Delta_1 = c_d \dot{\Delta}_2 = P_d \tag{2.12}$$

The deformations of the two elements are related to the total damper deformation Δ_d as follows

$$\Delta_1 + \Delta_2 = \Delta_d \tag{2.13}$$

Differentiating Eq. (2.13), we obtain,

$$\dot{\Delta}_1 + \dot{\Delta}_2 = \dot{\Delta}_d \tag{2.14}$$

Using the force relationships of Eq. (2.12) in Eq. (2.14), we obtain the following relating the force in the damper with the damper deformation

$$\frac{\dot{P}_d}{k_d} + \frac{P_d}{c_d} = \dot{\Delta}_d \tag{2.15}$$

We re-write this first order equation in the following standard form:

$$P_d(t) + \tau_d \dot{P}_d(t) = c_d \dot{\Delta}_d(t) \tag{2.16}$$

where, $\tau_d = c_d / k_d$ is referred to as the relaxation time constant.

It is of interest to examine the force deformation characteristics of this model. For this, consider the solution of this equation for a harmonic deformation as follows:

$$\Delta_d = \Delta_o \sin \omega t \tag{2.17}$$

The solution for this harmonic deformation with the zero-start initial condition can be written as:

$$P_d(t) = P_0 \frac{a}{1+a^2}\left[-e^{-\omega t/a} + \cos(\omega t) + a\sin(\omega t)\right] \tag{2.18}$$

where

$$a = \omega\tau_d \;\; ; \qquad P_0 = \Delta_0 k_d \tag{2.19}$$

The parametric Eqs. (2.17) and (2.18) can be used to create a force-deformation plot. Figure 2.3 shows these plots for different values of the parameter $a = \omega\tau_d$. The Figure clearly shows that the model shows increasing stiffness as the frequency of the deformation is increased for a fixed value of the relaxation time parameter. In the steady state situation, when the first term becomes insignificant the solution in Eq. (2.18) can be written as follows:

$$P_d(t) = \frac{\Delta_0 k_d a}{1+a^2}\left[\cos(\omega t) + a\sin(\omega t)\right] \tag{2.20}$$

Using Eq. (2.17) into Eq. (2.20), we obtain the following equation relating $P_d(t)$ with $\Delta_d(t)$:

$$\begin{aligned} P_d(t) &= \frac{k_d a^2}{1+a^2}\Delta(t) + \frac{c_d}{1+a^2}\dot{\Delta}(t) \\ &= k_e(a)\Delta(t) + c_e(a)\dot{\Delta}(t) \end{aligned} \tag{2.21}$$

where $k_e(a)$ and $c_e(a)$ are frequency dependent stiffness and damping coefficients of the model defined as:

$$k_e(a) = \frac{k_d a^2}{1+a^2}; \; c_e(a) = \frac{c_d}{1+a^2} \tag{2.22}$$

Figure 2.3 shows the variation of these equivalent coefficients with parameter a, which is the product of the frequency of deformation ω and relaxation time parameter τ_d. The equivalent stiffness coefficient increases with the frequency whereas the damping coefficient decreases with the frequency. One can also obtain the following nonparametric equation relating force with deformation by eliminating ωt between Eqs. (2.17) and (2.20):

$$\left(\frac{P}{P_0}\right)^2\left(\frac{1+a^2}{a}\right)^2-2\left(\frac{P}{P_0}\right)\left(\frac{\Delta}{\Delta_0}\right)\left(1+a^2\right)+\left(\frac{\Delta}{\Delta_0}\right)^2\left(1+a^2\right)=1$$

where

$$P_0=\Delta_0 k_d$$

This equation describes the ellipses, which were obtained in Figure 2.3 during the steady state situation.

A viscous damping device can also be modeled by a more complex combination of the springs and dashpots in parallel and series. One such model is called Wiechert model as shown in Figure 2.1(c). It finds applications in the devices exhibiting stiffness at very low frequencies. Bituminous fluid damper is one of its examples. The force in the device is obtained as:

$$P_d(t)+\tau_d\dot{P}_d(t)=\tau_d k_g\dot{\Delta}_d(t)+k_e\Delta_d(t) \tag{2.23}$$

where k_g and k_e are, respectively, the stiffness coefficients of the "glossy" and "rubbery" materials.

This study will focus only on the use of the Maxwell model for fluid viscous dampers. As indicated by Constantinou and Symans (1993), some commercially available dampers need to be characterized by this model. The following analytical development and subsequent analysis and numerical results are thus obtained only for dampers using this particular model. In the following we first develop the equations of motion and then their solution approach for the structures installed with such a dampers.

2.3 Equations of Motion with Maxwell Dampers

Substituting for $\dot{\Delta}_d$ in terms of structural response $\dot{\mathbf{x}}(t)$ from Eq. (2.3), we obtain the following equation for the damper force.

$$\tau_d \dot{P}_d(t) + P_d(t) - c_d \mathbf{r}_d^T \dot{\mathbf{x}}(t) = 0; \qquad d = 1, \ldots, n_l \tag{2.24}$$

Assembling these equations for individual dampers in matrix form we obtain:

$$\boldsymbol{\Gamma}\dot{\mathbf{P}}_d(t) - \mathbf{D}\dot{\mathbf{x}}(t) + \mathbf{P}_d(t) = \mathbf{0} \tag{2.25}$$

Where,

$$\mathbf{D} = \begin{bmatrix} c_1 \mathbf{r}_1^T \\ \vdots \\ c_{n_l} \mathbf{r}_{n_l}^T \end{bmatrix}; \ \boldsymbol{\Gamma} = \begin{bmatrix} \tau_1 & \cdots & 0 \\ \vdots & \ddots & \vdots \\ 0 & \cdots & \tau_{n_l} \end{bmatrix} \tag{2.26}$$

This equation can be combined with the equation of motion (2.1) to provide the following state space system of equation of the first order as:

$$\mathbf{A}_s \dot{\mathbf{z}}(t) + \mathbf{B}_s \mathbf{z}(t) = -\mathbf{D}_s \begin{Bmatrix} \mathbf{E} \\ \mathbf{0} \\ \mathbf{0} \end{Bmatrix} \ddot{X}_g(t) \tag{2.27}$$

where the system matrices $\mathbf{A}_s$, $\mathbf{B}_s$ and $\mathbf{D}_s$ are now of dimension $(2n + n_l) \times (2n + n_l)$, and are defined as:

$$\mathbf{A}_s = \begin{bmatrix} \mathbf{M} & \mathbf{0} & \mathbf{0} \\ \mathbf{0} & \mathbf{I} & \mathbf{0} \\ \mathbf{0} & \mathbf{0} & \boldsymbol{\Gamma} \end{bmatrix}; \ \mathbf{B}_s = \begin{bmatrix} \mathbf{C}_s & \mathbf{K}_s & \mathbf{L} \\ -\mathbf{I} & \mathbf{0} & \mathbf{0} \\ -\mathbf{D} & \mathbf{0} & \mathbf{I} \end{bmatrix}; \ \mathbf{D}_s = \begin{bmatrix} \mathbf{M} & \mathbf{0} & \mathbf{0} \\ \mathbf{0} & \mathbf{0} & \mathbf{0} \\ \mathbf{0} & \mathbf{0} & \mathbf{0} \end{bmatrix}; \ \mathbf{z}(t) = \begin{Bmatrix} \dot{\mathbf{x}}(t) \\ \mathbf{x}(t) \\ \mathbf{P}_d(t) \end{Bmatrix} \tag{2.28}$$

$$\mathbf{L} = \begin{bmatrix} n_1 \mathbf{r}_1 & \cdots & n_{n_l} \mathbf{r}_{n_l} \end{bmatrix} \tag{2.29}$$

Eq. (2.27) can be solved by a generalized modal analysis approach as has been done by Moreschi (2000). However, it is noted that the system matrix $\mathbf{B}_s$ is not symmetric and the system is not self-adjoint. In this case, one has to solve for both the right and left eigenvectors if a modal solution is desired. The gradient calculations that are required for the optimization analysis also become more complicated and cumbersome. It is therefore desirable to develop the symmetric equations of motion. In the following section we,

therefore, develop these symmetric equations of motion for the structures installed with Maxwell dampers using the Lagrange equations.

Symmetric Equations of Motion with Maxwell Dampers

To obtain the equations of motion in symmetric form, we will use the Lagrange equations. Consider a bay of a shear building in Figure 2.5 installed with a Maxwell damper. Assume that the damper is installed in a Chevron brace as shown in the Figure 2.5. One can also develop similar equations of motion for these dampers installed on other type of brace. Figure 2.5 shows the degrees of freedom associated with this system. In addition to the degrees of freedom representing the floor displacement, we have now introduced another degree of freedom to define the deformations of the spring and dashpot separately. In terms of these degrees of freedom, the kinetic energy, potential energy, and dissipation function can be expressed as follows:

$$T = \sum_{i=1}^{n} \frac{1}{2} m_i (\dot{x}_i + \dot{x}_g)^2 ;\; V = \sum_{i=1}^{n} \frac{1}{2} k_i (x_i - x_{i-1})^2 + \sum_{i=1}^{n} \frac{1}{2} k_{d_i} (x_{a_i} - x_{i-1})^2 \tag{2.30}$$

$$D = \sum_{i=1}^{n} \frac{1}{2} c_i (\dot{x}_i - \dot{x}_{i-1})^2 + \sum_{i=1}^{n} \frac{1}{2} c_{d_i} (\dot{x}_i - \dot{x}_{a_i})^2 ;\; x_0 = 0; \dot{x}_0 = 0 \tag{2.31}$$

where m_i, k_i and c_i, respectively, denote mass, inherent stiffness and inherent damping of i^{th} story; c_{d_i} and k_{d_i} represent damping and stiffness coefficient of the device in i^{th} story; x_i and $\dot{x}_i$ are the relative displacement and relative velocity of the i^{th} floor; and x_{a_i} and $\dot{x}_{a_i}$ are the displacement and velocity terms associated with an auxiliary degree of freedom.

The following Lagrange's equation is used to obtain the equation of motion for each degree of freedom.

$$\frac{d}{dt}\left(\frac{\partial T}{\partial \dot{q}_k} \right) - \frac{\partial T}{\partial q_k} + \frac{\partial V}{\partial q_k} + \frac{\partial D}{\partial \dot{q}_k} = 0 ; \qquad k = 1,...,n \tag{2.32}$$

where T represents total kinetic energy of the system, V is the total potential energy, and D, known as Raleigh dissipation function which takes into account damping forces which are assumed to be proportional to velocities.

Using Eq. (2.32) for the degree of freedom x_i associated with the i^{th} mass we obtain,

$$\begin{aligned} &m_i\ddot{x}_i + c_i(\dot{x}_i - \dot{x}_{i-1}) - c_{i+1}(\dot{x}_{i+1} - \dot{x}_i) + c_{d_i}(\dot{x}_i - \dot{x}_{a_i}) + \\ &k_i(x_i - x_{i-1}) - k_{i+1}(x_{i+1} - x_i) - k_{d_{i+1}}(x_{a_{i+1}} - x_i) = -m_i\ddot{x}_g \end{aligned} \tag{2.33}$$

or

$$\begin{aligned} &m_i\ddot{x}_i - c_i\dot{x}_{i-1} + (c_i + c_{i+1} + c_{d_i})\dot{x}_i - c_{i+1}\dot{x}_{i+1} - c_{d_i}\dot{x}_{a_i} - k_i x_{i-1} \\ &+(k_i + k_{i+1} + k_{d_{i+1}})x_i - k_{i+1}x_{i+1} - k_{d_{i+1}}x_{a_{i+1}} = -m_i\ddot{x}_g \end{aligned} \tag{2.34}$$

For the first floor mass and top floor mass, these equations are specialized as follows:

For $i = 1$,

$$m_1\ddot{x}_1 + (c_1 + c_2 + c_{d_1})\dot{x}_1 - c_2\dot{x}_2 - c_{d_1}\dot{x}_{a_1} + (k_1 + k_2 + k_{d_2})x_1 - k_2x_2 - k_{d_2}x_{a_2} = -m_1\ddot{x}_g \tag{2.35}$$

For $i = n$,

$$m_n\ddot{x}_n - c_n\dot{x}_{n-1} + (c_n + c_{d_n})\dot{x}_n - c_{d_n}\dot{x}_{a_n} - k_n x_{n-1} + k_n x_n = -m_n\ddot{x}_g \tag{2.36}$$

Similarly, using the Lagrange equation with the auxiliary degree of freedom x_{a_i} associated with the damper gives the following equation

$$-c_{d_i}(\dot{x}_i - \dot{x}_{a_i}) + k_{d_i}(x_{a_i} - x_{i-1}) = 0 \tag{2.37}$$

or

$$-c_{d_i}\dot{x}_i + c_{d_i}\dot{x}_{a_i} - k_{d_i}x_{i-1} + k_{d_i}x_{a_i} = 0 \tag{2.38}$$

Again writing this equation for $i = 1$ and $i = n$, respectively, we get

$$-c_{d_1}\dot{x}_1 + c_{d_1}\dot{x}_{a_1} + k_{d_1}x_{a_1} = 0 \tag{2.39}$$

$$-c_{d_n}\dot{x}_n + c_{d_n}\dot{x}_{a_n} - k_{d_n}x_{n-1} + k_{d_n}x_{a_n} = 0 \tag{2.40}$$

The equations of motion (2.34) and (2.38) can be combined into the matrix form as follows:

$$\mathbf{M}_s\ddot{\mathbf{x}}(t) + (\mathbf{C}_s + \mathbf{C}_d^{**})\dot{\mathbf{x}}(t) - \mathbf{C}_d^T\dot{\mathbf{x}}_a(t) + (\mathbf{K}_s + \mathbf{K}_d^{**})\mathbf{x}(t) - \mathbf{K}_d^T\mathbf{x}_a(t) = -\mathbf{M}_s\mathbf{E}\ddot{X}_g(t) \tag{2.41}$$

$$-\mathbf{C}_d\dot{\mathbf{x}}(t) + \mathbf{C}_d^*\dot{\mathbf{x}}_a(t) - \mathbf{K}_d\mathbf{x}(t) + \mathbf{K}_d^*\mathbf{x}_a(t) = \mathbf{0} \tag{2.42}$$

The vector $\mathbf{x}(t)$ contains the relative displacement values of the floor masses. The vector $\mathbf{x}_a(t)$ contains the relative displacement values associated with the auxiliary degrees of freedom introduced to define the deformation of the damper elements. $\mathbf{M}_s$, $\mathbf{C}_s$ and $\mathbf{K}_s$ are the usual mass, damping and stiffness matrices of the structure without the supplementary damping devices. The matrices $\mathbf{C}_d$, $\mathbf{C}_d^*$, $\mathbf{C}_d^{**}$, $\mathbf{K}_d$, $\mathbf{K}_d^*$ and $\mathbf{K}_d^{**}$ represent the contributions of the installed dampers to the system damping and stiffness matrices. These matrices as well the other matrices appearing in Eq. (2.41) are defined as follows.

$$\mathbf{C}_d^* = \begin{bmatrix} c_{d_1} & \cdots & 0 \\ \vdots & \ddots & \vdots \\ 0 & \cdots & c_{d_n} \end{bmatrix}_{n_a \times n_a} ; \mathbf{C}_d^{**} = \begin{bmatrix} c_{d_1} & \cdots & 0 \\ \vdots & \ddots & \vdots \\ 0 & \cdots & c_{d_n} \end{bmatrix}_{n \times n} ; \mathbf{C}_d = \begin{bmatrix} c_{d_1} & \cdots & 0 \\ \vdots & \ddots & \vdots \\ 0 & \cdots & c_{d_n} \end{bmatrix}_{n_a \times n} \tag{2.43}$$

$$\mathbf{K}_d^* = \begin{bmatrix} k_{d_1} & \cdots & 0 \\ \vdots & \ddots & \vdots \\ 0 & \cdots & k_{d_n} \end{bmatrix}_{n_a \times n_a} ; \mathbf{K}_d^{**} = \begin{bmatrix} k_{d_2} & 0 & 0 & 0 \\ \vdots & \ddots & \vdots & \vdots \\ 0 & \cdots & k_{d_n} & 0 \\ 0 & \cdots & 0 & 0 \end{bmatrix}_{n \times n} ;$$

$$\mathbf{K}_d = \begin{bmatrix} 0 & 0 & \cdots & 0 & 0 \\ k_{d_2} & 0 & \cdots & 0 & 0 \\ \vdots & \ddots & \ddots & \vdots & \vdots \\ 0 & 0 & \ddots & 0 & 0 \\ 0 & 0 & \cdots & k_{d_n} & 0 \end{bmatrix}_{n_a \times n} \tag{2.44}$$

Here $\mathbf{C}_d$, $\mathbf{C}_d^*$ and $\mathbf{C}_d^{**}$ are shown to be same. This will be the case if there is a damper in each story. However, if there is no damper in a story, then in matrix $\mathbf{C}_d^*$ the rows and columns associated with that damper are deleted, in $\mathbf{C}_d$ only the columns associated with the damper is deleted, and in $\mathbf{C}_d^{**}$ the element associated with the damper is set to zero without deleting the rows and columns.

To facilitate writing the equations of motion in the state space form, the following auxiliary equation is used

$$\mathbf{M}_s \dot{\mathbf{x}}(t) - \mathbf{M}_s \dot{\mathbf{x}}(t) = \mathbf{0} \tag{2.45}$$

Combining Eqs. (2.45), (2.42) and (2.41) in this order, we obtain the following system of first-order state equations:

$$\mathbf{A}\dot{\mathbf{z}}(t) + \mathbf{B}\mathbf{z}(t) = -\mathbf{D}\begin{Bmatrix}\mathbf{0}\\ \mathbf{0}\\ \mathbf{E}\end{Bmatrix}\ddot{X}_g(t) \tag{2.46}$$

where for an *n*-storied building, $\mathbf{z}(t)$ is the $2n + n_a$ - state vector consisting of the relative velocity vector $\dot{\mathbf{x}}(t)$, the vector of auxiliary variables $\mathbf{x}_a$ of dimension n_a, and the relative displacement vector $\mathbf{x}(t)$. This vector and the matrices $\mathbf{A}$, $\mathbf{B}$, $\mathbf{D}$ of dimension $2n + n_a \times 2n + n_a$ are defined as:

$$\mathbf{A} = \begin{bmatrix} \mathbf{0} & \mathbf{0} & \mathbf{M}_s \\ \mathbf{0} & \mathbf{C}_d^* & -\mathbf{C}_d \\ \mathbf{M}_s & -\mathbf{C}_d^T & \mathbf{C}_s + \mathbf{C}_d^{**} \end{bmatrix};\ \mathbf{B} = \begin{bmatrix} -\mathbf{M}_s & \mathbf{0} & \mathbf{0} \\ \mathbf{0} & \mathbf{K}_d^* & -\mathbf{K}_d \\ \mathbf{0} & -\mathbf{K}_d^T & \mathbf{K}_s + \mathbf{K}_d^{**} \end{bmatrix};\ \mathbf{D} = \begin{bmatrix} \mathbf{0} & \mathbf{0} & \mathbf{0} \\ \mathbf{0} & \mathbf{0} & \mathbf{0} \\ \mathbf{0} & \mathbf{0} & \mathbf{M}_s \end{bmatrix} \tag{2.47}$$

$$\mathbf{z}(t) = \begin{Bmatrix} \dot{\mathbf{x}}(t) \\ \mathbf{x}_a(t) \\ \mathbf{x}(t) \end{Bmatrix} \tag{2.48}$$

We note that all state matrices in Eq. (2.46) are symmetric. This will permit us to solve the equations using only one set of eigenvectors, as described in the following section.

2.4 Response Analysis

In the following chapter we will conduct an optimization study to calculate the optimum parameters of the chosen dampers. In this study we will need to calculate the response of Eq. (2.46) for seismic motion. We will also need to calculate the performance function and its gradients to perform the optimal search. In this section, therefore, we describe the response analysis approach that we have used in this study.

This solution approach is similar to the one mentioned in Section 2.2, and previously developed by Singh (1980). However, since the matrices involved are different in this system, the details are different. In the following we briefly describe the steps involved in the solution, and provide necessary equations that are used in this study. Since the matrices of the system are symmetric, we only need to calculate the right

eigenvectors to uncouple the system of equations. For this the following eigenvalue problem associated with Eq. (2.46) is solved:

$$-\mu_j \mathbf{A}\{\phi\}_j = \mathbf{B}\{\phi\}_j ; \; j = 1,\ldots,2n+n_a \tag{2.49}$$

where μ_j is the j^{th} eigenvalue and $\{\phi\}_j$ is the corresponding $2n+n_a$-dimensional eigenvector. The matrices $\mathbf{A}$ and $\mathbf{B}$ have been already defined in Eqs. (2.47). The eigenvectors and eigenvalues of Eq. (2.49) could be real or complex. The complex quantities will occur in the pairs of complex and conjugate. The real part of eigenvalues should be negative for a stable structural system.

To uncouple the system of equations, we use the following transformation of coordinates:

$$\mathbf{z}(t) = \mathbf{\Phi}\mathbf{y}(t) \tag{2.50}$$

where $\mathbf{\Phi}$ is the modal matrix containing the eigenvectors of the system. Using Eq. (2.50) and pre-multiplying Eq. (2.49) with the transpose of the modal matrix, we obtain the following $2n+n_a$ uncoupled equations for the principal coordinates $y_j(t)$.

$$\dot{y}_j(t) - \mu_j y_j(t) = -F_j \ddot{X}_g(t); \qquad j = 1,\ldots,2n+n_a \tag{2.51}$$

where F_j is the j^{th} participation factor and defined as:

$$F_j = \left\{\phi_j^{L/3}\right\}^T \mathbf{M}\,\mathbf{r}_g ; \; j = 1,\ldots,2n+n_a \tag{2.52}$$

$\phi_j^{L/3}$ is the part of j^{th} eigenvector $\{\phi\}_j$ containing lower n elements associated with $\mathbf{x}$ in the state vector and $\mathbf{r}_g$ is the vector of ground motion influence coefficients. Eq. (2.51) implicitly assumes that $\{\phi\}_j$ are normalized with respect to matrix $\mathbf{A}$. Although the general approach to obtain uncoupled equations (2.6) and (2.51) remain the same, the differences in the equations are noted. In the former case, $\{\phi\}_j$ had $2n$ elements whereas now it has $2n+n_a$ elements.

The solution of Eq. (2.51) can be found for any given ground motion description. This solution $y_j(t)$ can, then, be used to obtain any response quantity $R(t)$ of interest such as story displacement, story drift, and absolute floor acceleration, base shear, over

turning moment and others. A response quantity $R(t)$ is linearly related to the principal coordinate vector $y_j(t)$ as:

$$R(t) = \sum_{j=1}^{2n+n_a} \rho_j y_j(t) \tag{2.53}$$

in which ρ_j is the modal response of the quantity of interest. This modal response for a quantity of interest is related to eigenvector $\{\phi\}_j$ by linear transformation as

$$\rho_j = \mathbf{T}\{\phi_j\} \tag{2.54}$$

where **T** is the associated transformation vector. For various response quantities calculated in this study, this transformation vector **T** will be part of the following transformation matrices:

For Displacements of All Floors:

$$\mathbf{T}_x = \begin{bmatrix} \mathbf{0}_{n\times n} & \mathbf{0}_{n\times n_a} & \mathbf{I}_{n\times n} \end{bmatrix}_{n\times 2n+n_a} \tag{2.55}$$

For All Story Drifts:

$$\mathbf{T}_d = \begin{bmatrix} \mathbf{0}_{n\times n} & \mathbf{0}_{n\times n_a} & \mathbf{T}'_{n\times n} \end{bmatrix}_{n\times 2n+n_a}; \mathbf{T}' = \begin{bmatrix} 1 & 0 & 0 & \cdots & 0 \\ -1 & 1 & 0 & \ddots & \vdots \\ 0 & -1 & \ddots & \ddots & 0 \\ \vdots & \ddots & \ddots & \ddots & 0 \\ 0 & \cdots & 0 & -1 & 1 \end{bmatrix}_{n\times n} \tag{2.56}$$

For All Story Shears:

$$\mathbf{T}_s = \begin{bmatrix} \mathbf{0}_{n\times n} & \mathbf{0}_{n\times n_a} & \begin{bmatrix} \nwarrow & & \\ & k_{s_i} & \\ & & \searrow \end{bmatrix}_{n\times n} & \mathbf{T}'_{n\times n} \end{bmatrix}_{n\times 2n+n_a} \tag{2.57}$$

Base shear:

$$\mathbf{T}_b = \begin{bmatrix} \mathbf{0} \\ \mathbf{0} \\ \begin{Bmatrix} k_{s_1} \\ \vdots \\ 0 \end{Bmatrix} \end{bmatrix}^T_{2n+n_a \times 1} \tag{2.58}$$

Absolute Acceleration of all Floors:

$$\mathbf{T}_a = -\mathbf{M}_s^{-1}\left[\mathbf{C}_s + \mathbf{C}_d^{**} - \mathbf{C}_d{}^T\mathbf{C}_d^{*-1}\mathbf{C}_d \quad \mathbf{C}_d{}^T\mathbf{C}_d^{*-1}\mathbf{K}_d^* - \mathbf{K}_d^T \quad \mathbf{K}_s + \mathbf{K}_d^{**} - \mathbf{C}_d{}^T\mathbf{C}_d^{*-1}\mathbf{K}_d\right]_{n\times 2n+n_a} \tag{2.59}$$

Eq. (2.53) is used to define the time history of a response quantity. For earthquake motions defined in stochastic terms such as by a spectral density function or by design response spectra, we proceed as follows. Since the earthquake input motions can be considered as zero mean process, we first obtain the mean square value of the response. Assuming earthquake motions can be defined by a stationary random process, it can be shown (Maldonado and Singh, 1991) that the stationary mean square value of response $R(t)$ can be expressed as follows:

$$E\left[R^2(t)\right] = \int_{-\infty}^{\infty} \mathbf{\Phi}_g(\omega)\left[\sum_{j=1}^{2n+n_a}\sum_{k=1}^{2n+n_a}\left(\frac{q_j}{\mu_j - i\omega}\right)\left(\frac{q_j}{\mu_k + i\omega}\right)\right]d\omega \tag{2.60}$$

The quantity q_j is related to modal quantities as

$$q_j = \rho_j F_j = a_j + ib_j; \qquad j = 1,\ldots,2n+n_a \tag{2.61}$$

where a_j and b_j are the real and imaginary parts of q_j. For some eigenproperties, the imaginary part can also be zero as mentioned above. The quantity $\mathbf{\Phi}_g(\omega)$ in Eq. (2.60) represents spectral density function of the ground motion with ω being the frequency parameter.

To be able to use the earthquake input defined in terms of design ground response spectra, we must express the integral of Eq. (2.60) in terms of ground response spectra. This requires that we define Eq. (2.60) in terms of frequencies and damping ratios of

single degree of freedom oscillators representing the modes of the system. These parameters can be obtained from the complex and real eigenvalues of the system as described now. For each real eigenvalue and corresponding eigenvector we define the following quantities:

$$\alpha_j = \mu_j ;\ e_j = q_j ;\ \ j = 1,\ldots,n_r \tag{2.62}$$

where n_r is the number of real eigenproperties. To define the modal frequency and damping ratio associated with a pair of complex and conjugate eigenvalues, we express the real and imaginary parts of an eigenvalue as:

$$\left.\begin{aligned} &\omega_{j+n_r} = \left|\mu_{j+n_r}\right|;\ \ \beta_{j+n_r} = -\frac{\mathrm{Re}[\mu_{j+n_r}]}{\omega_{j+n_r}} \\ &\mu_{j+n_r} = -\beta_j\omega_j + i\omega_j\sqrt{1-\beta_j};\quad q_{j+n_r} = a_j + ib_j \end{aligned}\right\};\ \ j = 1,\ldots,n_c \tag{2.63}$$

Using these forms for the real and the complex and conjugate eigenvalues μ_j and modal quantities q_j in Eq. (2.63) and after some simplification one can express the mean square value of a response quantity as summation of three terms as follows:

$$E\left[R_i^2(\mathbf{c})\right] = S_{1i} + S_{2i} + S_{3i} \tag{2.64}$$

where the components of the quantities S_{1i}, S_{2i} and S_{3i} are defined as follows (Moreschi, 2000):

$$S_{1i} = \sum_{j=1}^{n_r} e_{ij}^2\, J_j + 2\sum_{j=1}^{n_r-1}\sum_{k=j+1}^{n_r} \frac{e_{ij}e_{ik}}{(\alpha_j + \alpha_k)}\left(\alpha_j J_j + \alpha_k J_k\right) \tag{2.65}$$

$$S_{2i} = 2\sum_{j=1}^{n_r}\sum_{k=1}^{n_r} e_{ij}\left(A_{jk}J_j + B_{jk}I_{1k} + C_{jk}I_{2k}\right) \tag{2.66}$$

$$S_{3i} = 2\sum_{j=1}^{n_c-1}\sum_{k=j+1}^{n_c}\left[W_{jk}\left(I_{1j} - \frac{I_{1k}}{\boldsymbol{\Omega}^4}\right) + Q_{jk}\left(I_{2j} - I_{2k}\right) + \frac{g_{ij}g_{ik}}{\boldsymbol{\Omega}^4}I_{1k} + 4a_{ij}a_{ik}I_{2k}\right] \tag{2.67}$$

Here, $\boldsymbol{\Omega}$ is the ratio of j^{th} and k^{th} system frequencies; and the quantities e_{ij}, a_{ij} and g_{ij} are defined in terms of the real and imaginary parts of the system eigenproperties.

The explicit expressions for W_{jk}, Q_{jk},…, were developed for the nonclassically damped case of Eqs. (2.66) and (2.67) by (Maldonado and Singh, 1991). Here they were obtained for the problem at hand, and are given in Appendix A . The terms J_j, I_{1j}, and I_{2j} in Eqs. (2.65), (2.66), and (2.67)are mean square values of the response quantities defined in terms of the input motion spectral density function as below:

$$J_j = \int_{-\infty}^{\infty} \frac{\mathbf{\Phi}_g(\omega)}{(\alpha_j^2 + \omega^2)} d\omega;$$

$$I_{1j} = \int_{-\infty}^{\infty} \frac{\mathbf{\Phi}_g(\omega)}{(\omega_j^2 - \omega^2) + 4\omega_j^2 \beta_j^2 \omega^2} d\omega;\ I_{2j} = \int_{-\infty}^{\infty} \frac{\mathbf{\Phi}_g(\omega)\omega^2}{(\omega_j^2 - \omega^2) + 4\omega_j^2 \beta_j^2 \omega^2} d\omega \quad (2.68)$$

It is noted that that I_{1j} and I_{2j} are the mean square value of the relative displacement and relative velocity responses, respectively of a single degree of freedom oscillator of parameters ω_j, β_j excited by ground motion component $\mathbf{f}(t)$. J_j represents the mean square response $E[\nu^2(t)]$ of the following first order equation

$$\dot{\nu}(t) + \alpha_j \nu(t) = \mathbf{f}(t) \quad (2.69)$$

The quantities I_{1j}, I_{2j} and J_j can also be defined in terms of the design ground response spectra. This will permit the use of the response spectra in the analysis as well as in the optimization study if desired.

2.5 Chapter Summary

The chapter focuses on the development of equations of motion for structures installed with supplementary damping devices modeled by Maxwell model. These equations being symmetric are more convenient for analysis than the unsymmetric equations used in earlier studies. The chapter ends with the description of the response analysis procedures to be used in the optimization algorithm in next chapter.

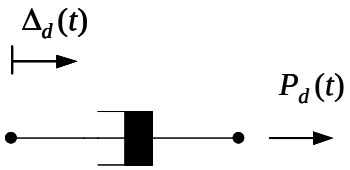

(a) Viscous Dashpot

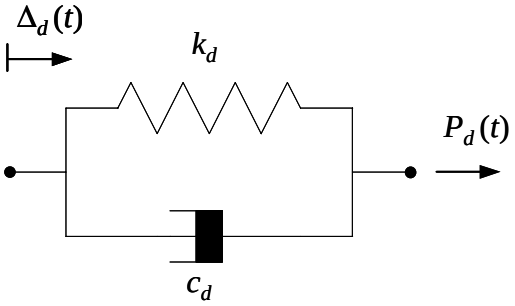

(b) Kelvin Model

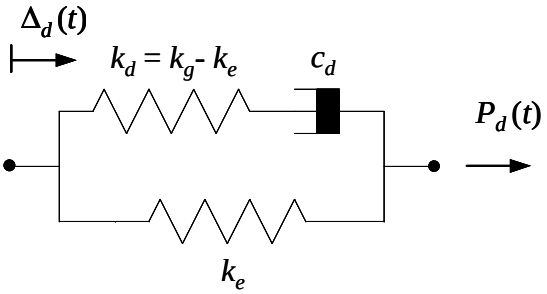

(c) Wiechert Model

Figure 2.1: Different Models for Viscous Dampers.

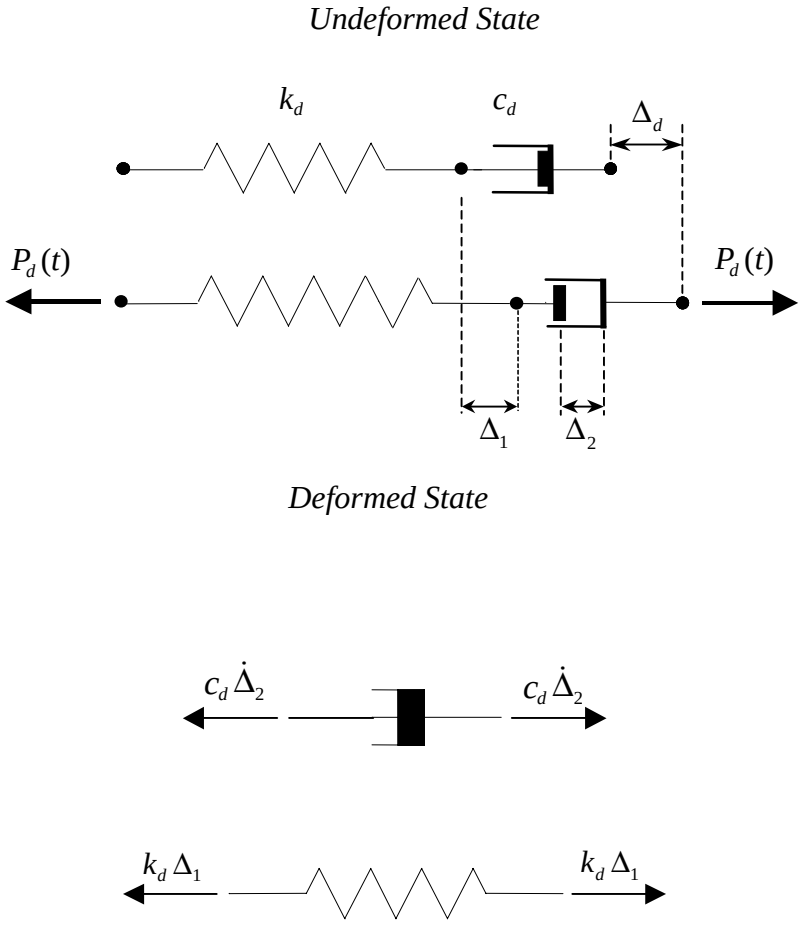

Figure 2.2: Maxwell Model of a Damping Device Representing the Deformations in the Spring and the Damping Element.

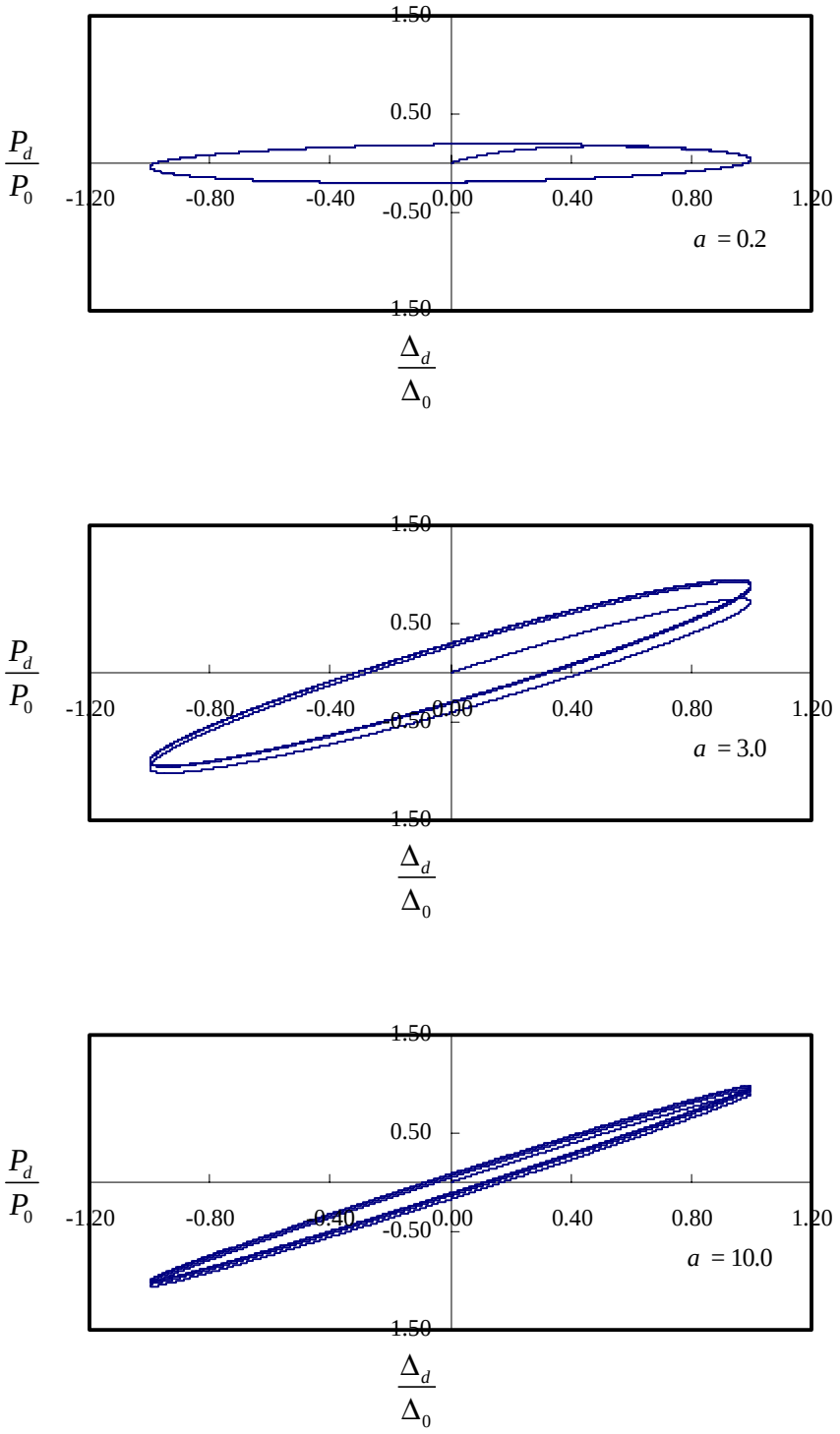

Figure 2.3: Force-Deformation Responses for Different Values of Parameter *a* (0.2, 3.0, 10.0).

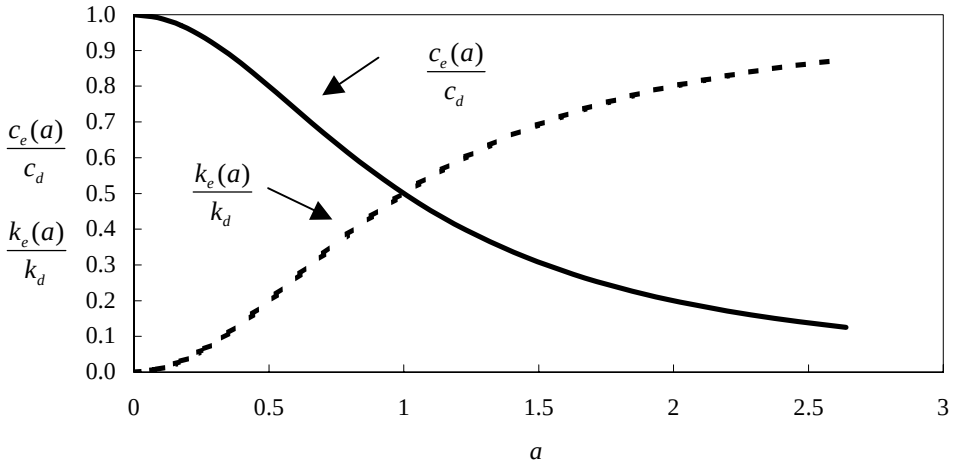

Figure 2.4: Frequency Dependency of the Stiffness and Damping Parameters.

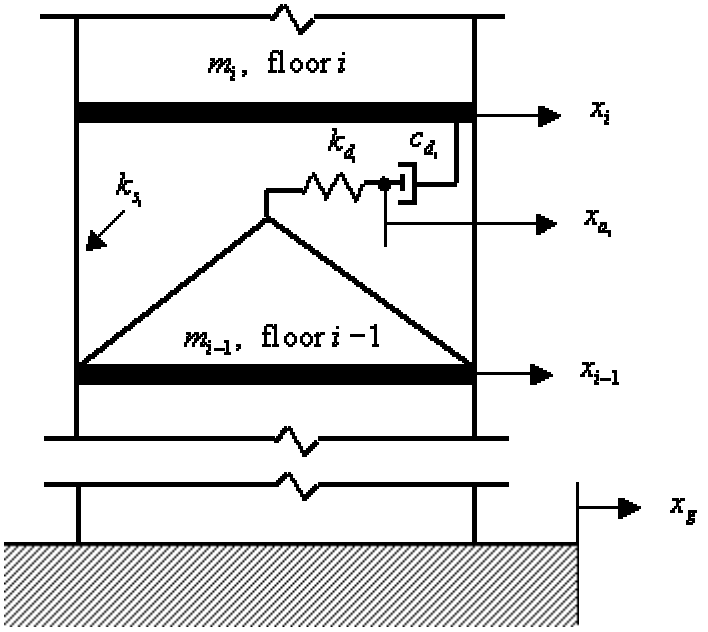

Figure 2.5: A Bay with Chevron Bracing Depicting Auxiliary DOF and Floor DOF for Floor *i.*

Chapter 3

Optimal Damper Parameters

3.1 Introduction

The main objective of installing supplementary dampers is to reduce the dynamic response such as the forces and acceleration of a structure. The level of response reduction will, however, depend on the location of damper installation and the damping force that damper can apply. Therefore, a question that naturally arises is how one should distribute these energy dissipation devices on the structure to reduce a response quantity optimally. One may also be interested in knowing the total amount of damping and its distribution in the structure so as to reduce a response quantity by a pre-decided amount in an optimal manner. A few different approaches have been suggested earlier to obtain better performance from the dampers. Hanson *et. al*, (1993) suggested the installation of devices to maximize damping in the first mode of the structure. Zhang and Soong (1992) used a sequential optimal scheme. In absence of any other clear choice, often a uniform distribution is assumed. This chapter deals with this issue as an optimization problem. The problem consists of a performance function that measures the desired attribute of the structure. The objective then is to minimize or maximize this function by optimal distribution of the parameters of the damping devices.

The development of optimization techniques or more formally called mathematical programming techniques dates back to the days of Newton, Lagrange, and Cauchy. However, the major developments in this area took place around the 1960s. Since then there has been a large amount of research in this field. Several optimization approaches and algorithms are available today. They are classified based on the nature of design variables, constraint equations and of course the objective function.

The chapter first describes the performance functions that have been considered in this study. It then formulates the optimization problem. A gradient-based approach called the Rosen's gradient projection method is selected to solve the problem at hand. A brief description of this approach, as it is applied to the problem of the optimal placement and parameter selection of the dampers, is then provided. The formulas to calculate the gradients of the response quantities and the eigenproperties required in the optimal search procedure are provided. This is followed by the numerical results of an example building structure, which illustrate the application of the proposed optimal approach.

3.2 Performance Functions

The performance objective that we want to achieve by installation of damping devices could be as simple as reduction of a specific response quantity such as a floor acceleration, floor displacement, base shear, overturning moment, *etc*. It could also involve more than one response quantity of similar type such as the sum of the squares of the floor accelerations or sum of the squares of the story drifts. It may also be a weighted average of different response quantities such floor accelerations and story drifts. More complex performance functions can also be chosen such as minimization of the life-cycle cost as it is influenced by the installation of the supplementary devices.

The performance function used in this work is in the form of normalized indices, called performance indices. The indices are defined in terms of response quantities of the structure installed with devices normalized by the corresponding response quantity for the structure without any additional devices. We shall use two forms of performance indices. The first form is where response quantities of interest like floor acceleration, drift or displacement of a particular story or base shear themselves represents the performance function. This performance function in its normalized form is give as follows:

$$f_1[R(\mathbf{c})] = \frac{R(\mathbf{c})}{R_o} \tag{3.1}$$

where $R(\mathbf{c})$ is the response quantity of interest. The goal is to minimize or reduce the maximum value of this quantity by using additional damping devices. The performance

function is normalized by the corresponding response quantity R_o of the original unmodified structure. In this study, this index shall be used for base shear response.

Another form of performance function is defined in terms of the second norm of a vector of response quantities, such as root mean square values of the story drifts, or acceleration of different floors, *etc*. This second form of performance function is expressed in normalized form as below:

$$f_2[\mathbf{R}(\mathbf{c})] = \frac{\|\mathbf{R}(\mathbf{c})\|}{\|\mathbf{R}_o\|} \tag{3.2}$$

where $\mathbf{R}(\mathbf{c})$ and $\mathbf{R}_o$, respectively, are the vectors of the response quantities of interest of the modified and unmodified structures; and $\|\mathbf{R}(\mathbf{c})\| = \sqrt{\sum_{i=1}^{n} R_i^2}$ and $\|\mathbf{R}_o\| = \sqrt{\sum_{i=1}^{n} R_{oi}^2}$ are the square roots of the second norm response of the modified and unmodified structures, respectively.

3.3 Formulation of Optimization Problem

The objective of the optimization study is to determine the parameter values of dampers, and also their distribution in the structure, to achieve the maximum reduction in the desired response measured in terms of a performance index. The parameter values are bounded by practical limits on them. Thus, the minimization of the performance function is to be obtained under constrained parameter values. Mathematically, this optimization problem can be posed as:

$$\text{Minimize } f(\mathbf{c}) \tag{3.3}$$

subject to

$$\sum_{i=1}^{n} c_i - C_T = 0 \tag{3.4}$$

$$0 \le c_i \le c_i^u \qquad i = 1,...,n \tag{3.5}$$

where $f(c)$ is the objective function or performance index, $\mathbf{c}$ is the vector containing design variables c_i, c_i^u is the upper bound value of the damping coefficient for the i^{th} damper, C_T is the total amount of damping coefficient value to be distributed in the

structure and *n* is the number of stories. Although, there are two parameters in a Maxwell damper - damping coefficient for the damping element and the stiffness coefficient for the spring element - here only the damping coefficient values are chosen as independent variables. This assumes that for a given damper, the stiffness coefficient is just a constant factor times the damping coefficient value.

It can be shown that the optimal solution of such a problem must satisfy the Kuhn-Tucker conditions (Rao, 1996). For the present problem, these conditions can be stated as follows:

$$\frac{\partial f(\mathbf{c}^*)}{\partial c_i} + \sum_{j \in A} \lambda_j = 0 \qquad i = 1, \ldots, n \tag{3.6}$$

$$\sum_{i=1}^{n} c_i - C_T = 0 \tag{3.7}$$

$$c_j = 0 \qquad j \in A \tag{3.8}$$

$$c_j - c_j^u = 0 \qquad j \in A \tag{3.9}$$

$$\lambda_j > 0 \qquad j \in A \tag{3.10}$$

where *A* represents the set of active constraints with the associated Lagrange multipliers λ_j, $\mathbf{c}^*$ is the vector containing design variables that minimizes the performance function.

Having defined the optimization problem, one needs to select an optimization technique to solve Eqs. (3.6) to (3.10). As mentioned earlier, Rosen's gradient projection method is a suitable technique for the present case. A brief description of this technique is now presented. The details can be found in literature (Rosen, 1960; Haftka and Gurdal, 1992; Rao, 1996).

As with many other gradient-based schemes, the technique is based on a step-by-step iterative procedure. Starting with an initial guess of the design variables, one successively updates the initial and subsequent estimates using the following recursive scheme:

$$\mathbf{c}_{k+1} = \mathbf{c}_k + \alpha_k \mathbf{s}_k \tag{3.11}$$

where $\mathbf{c}_k$ and $\mathbf{c}_{k+1}$ are the vectors of design variables at the k^{th} and $k+1^{th}$ step, α_k is the step length, and $\mathbf{s}_k$ is the search direction for succeeding estimate with k being the current iteration step. Thus to update the vector of design variables, we need two quantities: (1) the best search direction $\mathbf{s}_k$ and, (2) a largest possible step size α_k that will avoid instability in the search for the optimal solution.

The strategy is to approach the minimum of the function in the direction of steepest descent. Mathematically, it implies that the direction $\mathbf{s}_k$ must be such that it minimizes its scalar product with the gradient vector of the performance function of Eq. (3.3). Furthermore, the search for a feasible direction must be confined in the subspace defined by the active constraints. For this, the feasible direction must also be orthogonal to the gradients of the constraints of Eqs. (3.4) and (3.5). In case of no constraints, this steepest descent direction is the negative of gradient vector of the function. Since the present problem has constraints, the problem of finding a feasible direction can be stated as follows:

Find $\mathbf{s}_k$ which minimizes

$$\mathbf{s}_k^T \nabla f(\mathbf{c}) \tag{3.12}$$

subject to

$$\left(\nabla g_j\right)^T \mathbf{s}_k = 0 \; ; \qquad j = 1, ..., p \tag{3.13}$$

where ∇f and ∇g_j are the gradients of the performance index and j^{th} active constraint, defined as:

$$\nabla f(\mathbf{c}) = \left[\frac{\partial f}{\partial c_1} \quad \frac{\partial f}{\partial c_2} \quad \cdots \quad \frac{\partial f}{\partial c_n} \right]^T \tag{3.14}$$

$$\nabla g_j(\mathbf{c}) = \left[\frac{\partial g_j}{\partial c_1} \quad \frac{\partial g_j}{\partial c_2} \quad \cdots \quad \frac{\partial g_j}{\partial c_n} \right]^T ; \qquad j = 1, \ldots, p \tag{3.15}$$

with p being the number of active constrains. It is noted that the number of active constraints can change from one step to another. Eq. (3.13) ensures that the search

direction is orthogonal to the gradients of the active constraints. Eq. (3.13) can be written for all active constrains collectively as:

$$\mathbf{N}^T\mathbf{s}_k = 0 \tag{3.16}$$

where, the $n \times p$ matrix $\mathbf{N}$ contains all the gradient vectors of the constraints in its columns as follows:

$$\mathbf{N} = \begin{bmatrix} \nabla g_1 & \nabla g_2 & \cdots & \nabla g_p \end{bmatrix} \tag{3.17}$$

Furthermore, if the search direction is defined by a unit vector then,

$$\mathbf{s}_k^T\mathbf{s}_k - 1 = 0 \tag{3.18}$$

To solve this equality-constrained problem defined by Eqs. (3.12), (3.16), and (3.18) we define the Lagrangian function as follows

$$L(\mathbf{s}_i, \boldsymbol{\lambda}, \beta) = \mathbf{s}_i^T\nabla f(\mathbf{c}) + \boldsymbol{\lambda}^T\mathbf{N}^T\mathbf{s}_i + \beta(\mathbf{s}_i^T\mathbf{s}_i - 1) \tag{3.19}$$

where $\boldsymbol{\lambda}$ is the vector of Lagrange multipliers associated with the constraints of Eq. (3.16), and β is the Lagrange multiplier for the constraint of Eq. (3.18). The necessary conditions for the minimum are then obtained by setting to zero the first order partial derivatives of this function with respect to the components of the vector of search direction and the Lagrange multipliers. These conditions can be expressed as,

$$\frac{\partial L}{\partial \mathbf{s}_i} = \nabla f(\mathbf{c}) + \mathbf{N}^T\boldsymbol{\lambda} + 2\ \boldsymbol{\beta}\ \mathbf{s}_i = \mathbf{0} \tag{3.20}$$

$$\frac{\partial L}{\partial \boldsymbol{\lambda}} = \mathbf{N}^T\mathbf{s}_i = \mathbf{0} \tag{3.21}$$

$$\frac{\partial L}{\partial \boldsymbol{\beta}} = \mathbf{s}_i^T\mathbf{s}_i - 1 = \mathbf{0} \tag{3.22}$$

To solve these equations for the search direction vector $\mathbf{s}_k$ we proceed as follows. Premultiplying Eq. (3.20) by $\mathbf{N}^T$, and utilizing Eq. (3.21) gives

$$\mathbf{N}^T\nabla f(\mathbf{c}) + \mathbf{N}^T\mathbf{N}\boldsymbol{\lambda} = \mathbf{0} \tag{3.23}$$

Solving this for $\boldsymbol{\lambda}$, we obtain

$$\boldsymbol{\lambda} = -(\mathbf{N}^T\mathbf{N})^{-1}\mathbf{N}^T\nabla f \tag{3.24}$$

Substituting Eq. (3.24) into Eq. (3.20) gives

$$\mathbf{s} = -\frac{1}{2\beta}\mathbf{P}\nabla f \tag{3.25}$$

where **P** is referred to as the projection matrix. It is defined in terms of the gradient matrix of the constraints as:

$$\mathbf{P} = \left[\mathbf{I} - \mathbf{N}(\mathbf{N}^T\mathbf{N})^{-1}\mathbf{N}^T\right] \tag{3.26}$$

The scaling factor 2β can be dropped as $\mathbf{s}_i$ defines only the direction of search. It will be dropped automatically when the search direction is normalized according to Eq. (3.22) This normalized search direction $\mathbf{s}_i$ can be expressed as:

$$\mathbf{s}_k = \frac{\mathbf{P}\nabla f}{\|\mathbf{P}\nabla f\|} \tag{3.27}$$

It is evident from Eqs. (3.26) and (3.27) that the projection matrix **P** reduces to the identity matrix **I**, and search direction $\mathbf{s}_k$ becomes the steepest descent direction, if no constraints are active. The algorithm makes an implicit assumption that the constraints are linearly independent so that $\mathbf{N}^T\mathbf{N}$ is nonsingular and can be inverted to define unambiguously Eqs. (3.24) and (3.26). As explained by Rao (1996), there are other special situations that can occur to affect the above procedure. For example, if in a iterative step $\mathbf{s}_k$ becomes zero and some of the Lagrange multipliers are negative then one needs to ignore the constraints with the most negative Lagrange multiplier, and re-calculate the projection matrix to continue the search procedure.

Once the search direction $\mathbf{s}_k$ has been determined, the maximum permissible step α_k along this direction needs to be fixed. The step length has to be large enough to reach the minimum value in the least number of steps at the same time avoiding any violation of the previously inactive constraints. To find the step size which will not violate any previously inactive constraints, we calculate the step size values for each of these constraints such that they become active. We then choose the step size, which is minimum of these step sizes. To calculate the step size for each inactive constraint to

become active, we proceed as follows. Consider an inactive linear constraint expressed in a general form as:

$$g_j(\mathbf{c}+\alpha\mathbf{s}_i)=\sum_{i=1}^{n}a_{ij}c_i-b_j\le 0\,,\quad j=1,\ldots,m \tag{3.28}$$

where m is the total number of inactive constraints. At the next step of the search, Eq. (3.28) can be expressed as

$$g_j(\mathbf{c}+\alpha\mathbf{s}_i)=g_j(\mathbf{c})+\alpha\sum_{i=1}^{n}a_{ij}s_i\le 0\,;\quad j=1,\ldots,m \tag{3.29}$$

The step length that would make an originally inactive j^{th} constraint active can be determined as

$$g_j(\alpha_j)=g_j(\mathbf{c})+\alpha_j\sum_{i=1}^{n}a_{ij}s_i=0 \tag{3.30}$$

which yields

$$\alpha_j=-\frac{g_j(\mathbf{c})}{\sum_{i=1}^{n}a_{ij}s_i} \tag{3.31}$$

The maximum allowable step size is then obtained as,

$$\alpha_m=\min_{\alpha_j>0}(\alpha_j) \tag{3.32}$$

It is also possible that the function minimum may occur along $\mathbf{s}_k$ for a value smaller than this calculated minimum permissible step size. This will occur when the rate of change of the function with respect to α at α_m is positive. In such a case, the position of minimum should be located to determine the step size. This algorithm is described in the flowchart shown in Figure 3.1.

3.4 Gradient Calculations

In the gradient projection method described in the previous section, one moves along the direction of the steepest descent that satisfies the problem constraints to reach the optimum value. To implement this approach, it is necessary to calculate the rate of

change of performance indices and constraint functions with respect to the design parameters at each successive estimate of the design point. Since we intend to use the response analysis procedure described in the previous chapter, where the response quantities are defined in terms of the system eigenproperties, we must define the gradients of these quantities with respect to the design variables.

The method to calculate the gradients of the frequencies and eigenvector of an undamped system was first developed by Fox and Kapoor (1968). The same procedure was also extended to calculate the derivatives of the complex eigenvectors and eigenvalues which are required to analyze non-proportionally damped but symmetric system of equations by Ghafory-Ashtiany and Singh (1981). This formulation can now be adopted, as the system of equations to be analyzed here are also symmetric. The rate of change formulae specialized for the system equations and matrices described in Eq. (2.44) through (2.46) are provided below. The derivation of these formulae and further details on the rates of change of intermediate quantities that are required in the calculation of the following derivatives are provided in Appendix B.

Derivatives of eigenvectors:

$$\{\phi\}_{j,i} = \sum_{l=1}^{2n+n_a} a_{jl}\{\phi\}_l \tag{3.33}$$

with

$$a_{jl} = \begin{cases} -\frac{1}{2}\{\phi^L\}_j^T \mathbf{C}_{,i}\{\phi^L\}_j & \text{if } j = l \\ -\frac{1}{(\mu_l - \mu_j)}\left[\{\phi^L\}_l^T(\mu_j \mathbf{C}_{,i} + \mathbf{K}_{,i})\{\phi^L\}_j\right] & \text{if } j \neq l \end{cases} \tag{3.34}$$

where $()_{,i}$ is the derivative of a quantity w.r.t. c_{d_i}; $\{\phi^L\}_j$ denotes part of the j^{th} eigenvector carrying lower $n_a + n$ elements and

$$\mathbf{C} = \begin{bmatrix} \mathbf{C}_d^* & -\mathbf{C}_d \\ -\mathbf{C}_d^T & \mathbf{C}_s + \mathbf{C}_d^{**} \end{bmatrix};\ \mathbf{K} = \begin{bmatrix} \mathbf{K}_d^* & -\mathbf{K}_d \\ -\mathbf{K}_d^T & \mathbf{K}_s + \mathbf{K}_d^{**} \end{bmatrix} \tag{3.35}$$

Derivatives of eigenvalues:

$$\mu_{j_{,i}} = -\{\phi^L\}_j^T(\mu_j \mathbf{C}_{,i} + \mathbf{K}_{,i})\{\phi^L\}_j \tag{3.36}$$

Derivatives of natural frequencies:

$$\omega_{j,i} = \frac{1}{\omega_j}\left\{\mathrm{Re}[\mu_j]\,\mathrm{Re}[\mu_{j,i}] + \mathrm{Im}[\mu_j]\,\mathrm{Im}[\mu_{j,i}]\right\} \tag{3.37}$$

Derivatives of modal damping:

$$\beta_{j,i} = \frac{1}{\omega_j^2}\left\{\mathrm{Re}[\mu_j]\omega_{j,i} + \omega_j\,\mathrm{Re}[\mu_{j,i}]\right\} \tag{3.38}$$

The operators Re[] and Im[] denote the real and imaginary parts of the complex number in the square bracket. In terms of these rates of change, the derivative of the i^{th} root mean square response component, $E[\mathbf{R}_i(\mathbf{c})]$, with respect to the i^{th} design variable can be obtained as

$$\{E[\mathbf{R}_i(\mathbf{c})]\}_{,i} = \frac{\{E[\mathbf{R}_i^2(\mathbf{c})]\}_{,i}}{\{E[\mathbf{R}_i(\mathbf{c})]\}} \tag{3.39}$$

where

$$\left\{E\left[\mathbf{R}_i^2(\mathbf{c})\right]\right\}_{,i} = (S_{1i} + S_{2i} + S_{3i})_{,i} \tag{3.40}$$

The detailed expressions for the rate of change of various intermediate quantities are given in Appendix C.

3.5 Numerical Results

Building Structure Model

To demonstrate the application of the above formulation, in this section we will present several sets of numerical results. A 24-story shear building has been considered for the installation of viscous dampers to reduce its response and improve its seismic performance. The physical properties of the building model are the same as in the study by Singh and Moreschi (2000) and Moreschi (2000). The mass is assumed concentrated at each floor level, and there is one degree of freedom associated with each floor mass. The mass and stiffness properties of this structure vary along the height and are given Table 3.1. The last column of this table also provides the modal frequencies. To incorporate the inherent energy dissipation that is usually present in the civil structures, a

modal damping ratio of 3% in each mode is assumed. This modal damping ratio value is used to construct the damping matrix for the system of Eq. (2.1).

Supplementary Dampers

The inherent damping is further supplemented by the installation of viscous damping devices. The supplementary dampers are represented by the Maxwell model with the relaxation time constant of 0.014 s. This parameter value is based on the experimental data reported by Reinhorn *et. al*, (1995). The results for other values for this parameter have also been reported to study the effect of this on passive response control. The procedure to calculate the total amount of damping needed to obtain a desired reduction in the response or a performance index is also discussed with numerical examples. The total supplemental damping installed on the structure is measured by the sum of the damping coefficients c_{d_i} at all locations.

Performance Indices

As mentioned earlier, herein the numerical results are obtained for three different performance indices used in the optimization study: (1) the base-shear index of Eq. (3.1), (2) the story drift-based performance index of Eq. (3.2) and, (3) the floor acceleration-based performance index of Eq. (3.2).

Seismic Input

The current formulation can handle the seismic input to the structure defined in two different forms: (1) a set of design response spectra, or (2) a spectral density function. In this study, the last form of the input is used. However, as mentioned earlier, the response formulation in Chapter 3 can also be used equally effectively with the input defined by response spectra. The expression of the input power spectral density function $\mathbf{\Phi}_g(\omega)$ used in this study is as follows:

$$\mathbf{\Phi}_g(\omega) = S \frac{\omega_g^4 + 4\ \beta_g^2\ \omega_g^2\ \omega^2}{(\omega_g^2\ -\omega^2)^2 + 4\ \beta_g^2\ \omega_g^2\ \omega^2} \tag{3.41}$$

This is the well-known Kanai-Tajimi spectral density function (Kanai, 1961; Tajimi, 1960) with parameters ω_g, β_g and S. These parameters can be established for site-specific ground motion characteristics. The values of the parameters ω_g, β_g and S used

in this study are 18.85 rad/s, 0.65, and 0.0619 m^2/s^3/rad, respectively. For this set of parameter values, Figure 3.2 shows this power spectral density function.

A Computational Issue

While using the optimization algorithm discussed earlier, it was observed that at some intermediate step, the calculated values of the parameters of one or more dampers became very small, that is nearly zero. As a result, one or more rows and columns in **C** and **K** matrices of Eq. (3.35) became zero. This rendered these matrices singular and caused numerical problems in the calculation of the system eigenproperties. To circumvent this computational difficulty, the rows and columns corresponding to zero damping coefficient values were deleted and thus the order of equations for the next optimization step was reduced. This procedure was found to be analytically consistent as the matrices with deleted rows and columns were the same as the matrices with no dampers at those locations.

3.5.1 Damping Distributions for Different Indices

First we present the results for the optimization with the drift-based index of Eq. (3.2). Here it is desired to reduce the drift-based index by 40% by optimal distribution of viscoelastic devices. That is, the performance index is to be reduced to a value of 0.6. We need to calculate the total amount of damping C_T in Eq. (3.4). First we guess the initial value of this coefficient to start the process. Here an initial value of $C_T = 1.10 \times 10^9$ N-s/m was assumed. This total damping was then distributed uniformly in different stories of the building to start the optimization process. This initial distribution was then refined by the optimization scheme presented in Section 3.2 to obtain the best value of the index with this damping. This optimal distribution is presented in Column (2) of Table 3.2. For each story, the results for the calculated design variables c_d^* are expressed as percentages of the total damping C_T. The magnitude of the reduction in the performance function achieved by this distribution of damping is shown in the last two rows of the table. It is seen that the desired reduction of 40% could not be achieved with the chosen amount of damping C_T. Thus, this total amount must be increased.

To estimate the additional amount of damping needed, we need to know the rate at which this performance function will change with a change in the total damping. That

is we need to calculate $\frac{\partial f}{\partial C_T}$. This can then be used to estimate the change in the coefficient value required to obtain the desired function using the following first order Taylor expansion:

$$f(C_T + \Delta C_T) = f(C_T) + \frac{\partial f(C_T)}{\partial C_T}\Delta C_T \tag{3.42}$$

Setting the function value at $C_T + \Delta C_T$ to the desired value $f(\mathbf{c}^*)$ of the optimum performance index, we obtain the following for the increment required in C_T:

$$\Delta C_T = -\frac{f_c(\mathbf{c}^*) - f(C_T)}{\frac{\partial f}{\partial C_T}} \tag{3.43}$$

The partial derivative in the denominator can be easily obtained by differentiating the Lagrangian associated with the optimal problem of Eqs. (3.3), (3.4), and (3.5) with respect to C_T. It will be immediately clear then that this partial derivative is merely the Lagrange multiplier associated with the constraint of Eq. (3.4). This multiplier is available as a by-product of the optimization process.

This new estimate of the total damping is then re-distributed to obtain the optimal distribution. The corresponding performance function, however, may not be exactly equal to the desired value. Further refinements may be made to obtain a better estimate of the total damping using Eq. (3.43), followed by the optimal re-distribution of this value, till a satisfactory convergence to the desired performance function value is achieved.

This process was used to calculate the final damping distribution required for a performance index of 0.6. The results in the next two columns show the result obtained after first increment of the damping calculated with the help of Eq. (3.43). The last row in the table again shows the performance index value achieved with this increased value of total damping. It is seen to be approaching the desired value of 0.6. Repeating the process once more provides the results shown in the last two columns of Table 3.2. It is seen that the performance index in this iteration is equal to the desired value.

For this final design, the evolution of the performance function with each iteration is plotted in Figure 3.3. The discontinuous horizontal line indicates the result for uniform

distribution of the devices. About 7.7% improvement over uniform distribution of damping is achieved which can be attributed to optimization process.

It is quite likely that the solution achieved as a result of gradient projection technique might not be globally optimal. To verify this, several initial guesses for distribution of total damping were made and the solutions obtained were in close proximity as shown in Table 3.3.

The same approach was used to calculate the optimal damping values required for reducing the acceleration-based performance index. These results are shown in Table 3.4. An intuitive guess of $C_T = 4.14\times10^8$ N-s/m was used for this performance function in the optimization problem. Using Eq. (3.43) one more time, the total damping value of $C_T = 4.60\times10^8$ N-s/m was found necessary to get the performance index value of 0.6036, or a reduction of 39.64% in the acceleration-based performance index.

Similar results obtained for the base shear performance index are shown in Table 3.5.

3.5.2 Effect of Using the Maxwell Model

We present the following results to examine what effect it would have if the series spring in the Maxwell model were ignored and the damper was simply modeled as a classical, velocity proportional damper. Corresponding to the three optimal designs shown in Tables 3.2, 3.4 and 3.5, new optimal designs were obtained assuming that the total damping values given in the last columns were provided by classical, velocity proportional dampers. The results are compared in Table 3.6 and 3.7. Table 3.6 is for $\tau_d = 0.014$ and Table 3.7 for $\tau_d = 0.14$. It is noted that the presence of a spring in series in the Maxwell model reduces the damping effectiveness and this effect is more pronounced for higher values of the relaxation time parameter τ_d. Thus ignoring the frequency-dependent stiffening effect in viscous dampers, could lead to unconservative designs if relaxation time parameter value is large. Figure 3.4 and 3.5, respectively, compares the reduction in drift, acceleration and base shear response in different stories for $\tau_d = 0.014$ s and $\tau_d = 0.14$ s.

Another simple study in connection with this examines the effect of τ_d on performance index. The drift and acceleration based performance indices were calculated for uniform distribution of $C_T = 1.32 \times 10^9$ N-s/m with varying values of relaxation constant τ_d. It is observed in Figure 3.6 that both the performance indices increase as the value of τ_d goes up. This signifies that the effectiveness of the damper decreases with increasing τ_d value.

3.5.3 Cross-effectiveness of the Drift-Based and Acceleration-Based Designs

The design based on reducing a performance index may also be effective in reducing another index or other response quantities. For example, a drift-based design although focused on reducing the drift response, may also be effective in reducing the acceleration response. It is thus of interest to compare the cross-effectiveness of the two or more designs. To examine this, in Figure 3.6 we have plotted the percent reductions in the story drifts and floor accelerations achieved in the drift-based and acceleration-based optimal designs. In both designs the total damping was fixed. In the drift-based design the optimal distribution was obtained to minimize the drift-based index, whereas in the acceleration-based design the distribution was obtained to minimize the acceleration index. Here Design I represents the optimal parameter values based on 40% reduction in drift-based objective function. For the Design II, the total damping obtained from Design I is re-distributed in optimal manner to achieve the maximum reduction in the floor acceleration based performance function. The reduction in base shear response resulting from two designs is also shown. We observe that drift reduction for the drift-based performance index design is more than that for the acceleration-based performance index design and vice-versa.

3.6 Chapter Summary

The Chapter formulates the problem for the optimal design and distribution of viscous dampers in structures to achieve certain performance objectives. The performance objectives are measured in terms of performance indices. These performance indices depend on the structural response, and the objective may be to minimize the performance

index to achieve a best reduction in the response represented by the index. The three different performance indices used in this study are described. The optimal solution is obtained by the Rosen's method which is known to be suitable for minimizing nonlinear performance functions with linear constrains. The approach requires the calculation of gradients of the performance index which in turn requires the gradients of the system eigenproperties. The approach for the calculation of these gradients is described. In the end, several sets of numerical results are presented to demonstrate the application of the optimal search approach. The numerical results also examine the effectiveness of such optimal designs in controlling the structural response.

Table 3.1: Properties of 24-Story Building

Story Mode (1)	***Mass [kg $\times 10^5$] (2)***	***Stiffness [N/m $\times 10^8$] (3)***	***Frequencies [rad/s] (4)***
1	74.26	20.98	3.43
2	74.26	19.77	8.30
3	69.18	18.55	13.39
4	69.70	18.55	18.26
5	58.49	17.41	23.14
6	55.87	17.29	28.27
7	55.69	17.29	32.96
8	40.63	16.09	37.74
9	36.78	15.81	41.34
10	36.78	15.81	45.76
11	36.78	15.67	50.01
12	34.15	15.55	54.30
13	34.15	15.55	57.59
14	28.55	14.92	61.60
15	24.69	14.75	64.97
16	24.69	14.75	68.89
17	23.29	14.55	74.26
18	17.69	14.34	78.24
19	17.69	14.34	83.06
20	15.24	13.45	87.97
21	12.78	13.38	93.24
22	12.61	13.45	98.51
23	9.28	13.43	107.43
24	7.71	13.96	116.54

Note: 3% modal damping ratio for all modes.

Table 3.2: Numerical Results Showing Incremental Refinement of the Total Damping Coefficient and its Distribution to Obtain a Given Value of Drift Based Performance Index

Story	$C_T = 1.10\times10^9$ ***N-s/m***	$C_T = 1.29\times10^9$ ***N-s/m***	$C_T = 1.32\times10^9$ ***N-s/m***
	c_d^* ***[% of*** C_T ***]***	c_d^* ***[% of*** C_T ***]***	c_d^* ***[% of*** C_T ***]***
(1)	(2)	(3)	(4)
1	0.00	0.00	0.00
2	0.00	0.00	0.00
3	0.00	0.00	0.00
4	0.00	0.00	0.00
5	0.00	0.00	0.00
6	0.00	0.00	0.00
7	0.00	0.00	0.00
8	0.00	1.04	1.06
9	5.66	6.14	6.24
10	2.97	3.89	3.97
11	0.00	1.38	1.43
12	3.19	3.53	3.60
13	0.00	0.00	0.00
14	8.03	8.24	8.33
15	13.81	13.55	13.64
16	8.35	8.46	8.50
17	6.68	7.00	7.06
18	16.05	16.35	16.26
19	10.50	10.41	10.36
20	9.75	9.03	8.87
21	8.61	7.13	6.94
22	3.63	2.07	2.02
23	2.75	1.78	1.74
24	0.00	0.00	0.00
$f(\mathbf{c}^*)$	0.62872	0.60373	0.60000
Reduction [%]	37.13	39.63	40.00

Table 3.3: Optimal Designs Obtained for Different Initial Guesses for $C_T = 1.32\times10^9$ N-s/m

Story	***Guess 1***	***Guess 2***	***Guess 3***	***Guess 4***	***Guess 5***
	c_d^* ***[% of*** C_T ***]***	c_d^* ***[% of*** C_T ***]***	c_d^* ***[% of*** C_T ***]***	c_d^* ***[% of*** C_T ***]***	c_d^* ***[% of*** C_T ***]***
1	0.00	0.00	0.00	0.00	0.00
2	0.00	0.00	0.00	0.00	0.00
3	0.00	0.00	0.00	0.00	0.00
4	0.00	0.00	0.00	0.00	0.00
5	0.00	0.00	0.00	0.00	0.00
6	0.00	0.00	0.00	0.00	0.00
7	0.00	0.00	0.00	0.00	0.00
8	0.00	2.14	0.00	1.06	0.00
9	8.37	3.89	3.62	6.24	6.14
10	2.81	5.14	5.96	3.97	2.14
11	0.97	0.00	2.86	1.43	4.24
12	3.10	5.07	6.31	3.60	5.02
13	0.00	1.04	2.09	0.00	7.03
14	7.99	6.86	6.95	8.33	6.47
15	13.61	13.49	13.72	13.64	9.74
16	8.57	7.74	6.86	8.50	7.59
17	6.56	6.99	7.24	7.06	8.11
18	15.00	16.10	13.19	16.26	12.88
19	10.41	9.75	9.20	10.36	8.93
20	8.03	9.65	8.72	8.87	8.47
21	7.71	7.13	7.77	6.94	7.45
22	3.38	3.23	2.72	2.02	3.54
23	3.63	1.79	2.79	1.74	2.27
24	0.00	0.00	0.00	0.00	0.00
$f(\mathbf{c}^*)$	0.5986	0.5998	0.5994	0.6000	0.6008
Reduction [%]	40.14	40.02	40.06	40.00	39.92

Table 3.4: Numerical Results Showing Incremental Refinement of the Total Damping Coefficient and its Distribution to Obtain a Given Value of Acceleration Based Performance Index

Story	$C_T = 4.14\times10^8$ ***N-s/m***	$C_T = 4.60\times10^8$ ***N-s/m***
	c_d^* ***[% of*** C_T ***]***	c_d^* ***[% of*** C_T ***]***
(1)	(2)	(3)
1	0.00	0.00
2	1.14	1.18
3	1.38	1.42
4	1.21	1.23
5	1.40	1.43
6	1.41	1.47
7	1.29	1.29
8	2.37	2.40
9	2.90	2.93
10	2.90	2.76
11	2.30	2.45
12	3.70	3.58
13	2.44	2.45
14	3.80	3.87
15	4.52	4.28
16	4.90	5.12
17	4.52	4.04
18	7.24	7.58
19	5.61	5.37
20	7.83	7.91
21	8.85	9.18
22	11.01	10.31
23	11.81	12.33
24	5.46	5.41
$f(\mathbf{c}^*)$	0.6085	0.6036
Reduction [%]	39.15	39.64

Table 3.5: Numerical Results Showing Incremental Refinement of the Total Damping Coefficient and its Distribution to Obtain a Given Value of Base Shear Based Performance Index

Story	$C_T = 4.60\times10^8$ ***N-s/m***	$C_T = 3.81\times10^8$ ***N-s/m***	$C_T = 3.88\times10^8$ ***N-s/m***
	c_d^* ***[% of*** C_T ***]***	c_d^* ***[% of*** C_T ***]***	c_d^* ***[% of*** C_T ***]***
(1)	(2)	(3)	(4)
1	0.00	0.00	0.00
2	0.00	0.00	0.00
3	0.00	0.00	0.00
4	0.00	0.00	0.00
5	0.13	0.00	0.00
6	0.00	0.00	0.00
7	0.00	0.00	0.00
8	2.07	1.17	1.63
9	2.21	0.00	2.49
10	2.41	1.44	2.32
11	2.12	1.47	2.12
12	2.59	2.53	3.23
13	2.64	0.97	1.95
14	3.68	2.76	3.25
15	5.77	6.33	5.32
16	6.72	6.52	6.50
17	5.48	5.64	5.05
18	6.75	6.91	6.46
19	9.38	10.09	9.07
20	10.10	11.06	9.56
21	11.44	12.93	11.68
22	12.21	13.48	13.24
23	8.89	10.54	9.93
24	5.41	6.17	6.18
$f(\mathbf{c}^*)$	0.5796	0.60213	0.60209
Reduction [%]	42.04	39.787	39.791

Table 3.6: Comparision of Results for Maxwell and Classical Models for τ_d = 0.014

Story	$C_T = 1.32\times10^9$ ***N-s/m***		$C_T = 4.60\times10^8$ ***N-s/m***		$C_T = 3.88\times10^8$ ***N-s/m***	
	c_d^* [% of C_T]		c_d^* [% of C_T]		c_d^* [% of C_T]	
	Drift		***Acceleration***		***Base Shear***	
	Maxwell	***Classical***	***Maxwell***	***Classical***	***Maxwell***	***Classical***
1	0.00	0.00	0.00	0.30	0.00	0.00
2	0.00	0.00	1.18	0.15	0.00	0.00
3	0.00	0.00	1.42	0.38	0.00	0.00
4	0.00	0.00	1.23	0.24	0.00	0.00
5	0.00	0.00	1.43	0.55	0.00	0.00
6	0.00	0.00	1.47	0.63	0.00	0.66
7	0.00	0.00	1.29	0.00	0.00	0.73
8	1.06	2.03	2.40	1.56	1.63	1.45
9	6.24	4.46	2.93	2.42	2.49	1.84
10	3.97	3.08	2.76	1.97	2.32	2.27
11	1.43	2.59	2.45	1.70	2.12	2.70
12	3.60	4.65	3.58	2.17	3.23	3.83
13	0.00	0.00	2.45	2.85	1.95	2.00
14	8.33	7.56	3.87	1.48	3.25	0.94
15	13.64	13.55	4.28	5.26	5.32	3.89
16	8.50	8.67	5.12	4.13	6.50	7.46
17	7.06	6.47	4.04	3.23	5.05	4.77
18	16.26	16.16	7.58	8.65	6.46	6.82
19	10.36	10.68	5.37	6.27	9.07	7.79
20	8.87	9.55	7.91	8.37	9.56	10.30
21	6.94	7.49	9.18	11.42	11.68	11.96
22	2.02	2.14	10.31	11.78	13.24	13.03
23	1.74	0.92	12.33	16.20	9.93	10.47
24	1.93	0.00	5.41	8.28	6.18	7.10
$f(\mathbf{c}^*)$	0.6000	0.5980	0.6036	0.5924	0.6021	0.5947

Table 3.7: Comparision of Results for Maxwell and Classical Models for τ_d = 0.14

Story	$C_T = 1.32\times10^9$ ***N-s/m***		$C_T = 4.60\times10^8$ ***N-s/m***		$C_T = 3.88\times10^8$ ***N-s/m***	
	c_d^* [% of C_T]		c_d^* [% of C_T]		c_d^* [% of C_T]	
	Drift		***Acceleration***		***Base Shear***	
	Maxwell	***Classical***	***Maxwell***	***Classical***	***Maxwell***	***Classical***
1	0.00	0.00	0.28	0.30	0.00	0.00
2	0.00	0.00	0.00	0.15	0.00	0.00
3	0.00	0.00	0.15	0.38	0.00	0.00
4	0.00	0.00	0.23	0.24	0.00	0.00
5	0.00	0.00	0.72	0.55	0.00	0.00
6	0.00	0.00	0.88	0.63	0.00	0.66
7	0.00	0.00	0.85	0.00	0.00	0.73
8	1.01	2.03	2.10	1.56	0.00	1.45
9	5.94	4.46	2.60	2.42	0.00	1.84
10	3.60	3.08	2.47	1.97	0.00	2.27
11	1.04	2.59	2.30	1.70	0.00	2.70
12	3.12	4.65	2.57	2.17	0.00	3.83
13	0.00	0.00	2.39	2.85	0.00	2.00
14	8.00	7.56	3.46	1.48	0.00	0.94
15	13.06	13.55	4.52	5.26	2.78	3.89
16	8.74	8.67	4.19	4.13	4.15	7.46
17	7.33	6.47	4.39	3.23	6.20	4.77
18	14.62	16.16	7.23	8.65	9.12	6.82
19	9.70	10.68	6.49	6.27	11.90	7.79
20	8.82	9.55	8.09	8.37	14.34	10.30
21	7.15	7.49	10.85	11.42	15.51	11.96
22	3.12	2.14	10.14	11.78	15.72	13.03
23	2.80	0.92	13.86	16.20	12.60	10.47
24	1.93	0.00	9.24	8.28	7.68	7.10
$f(\mathbf{c}^*)$	0.6670	0.5980	0.8127	0.5924	0.8005	0.5947

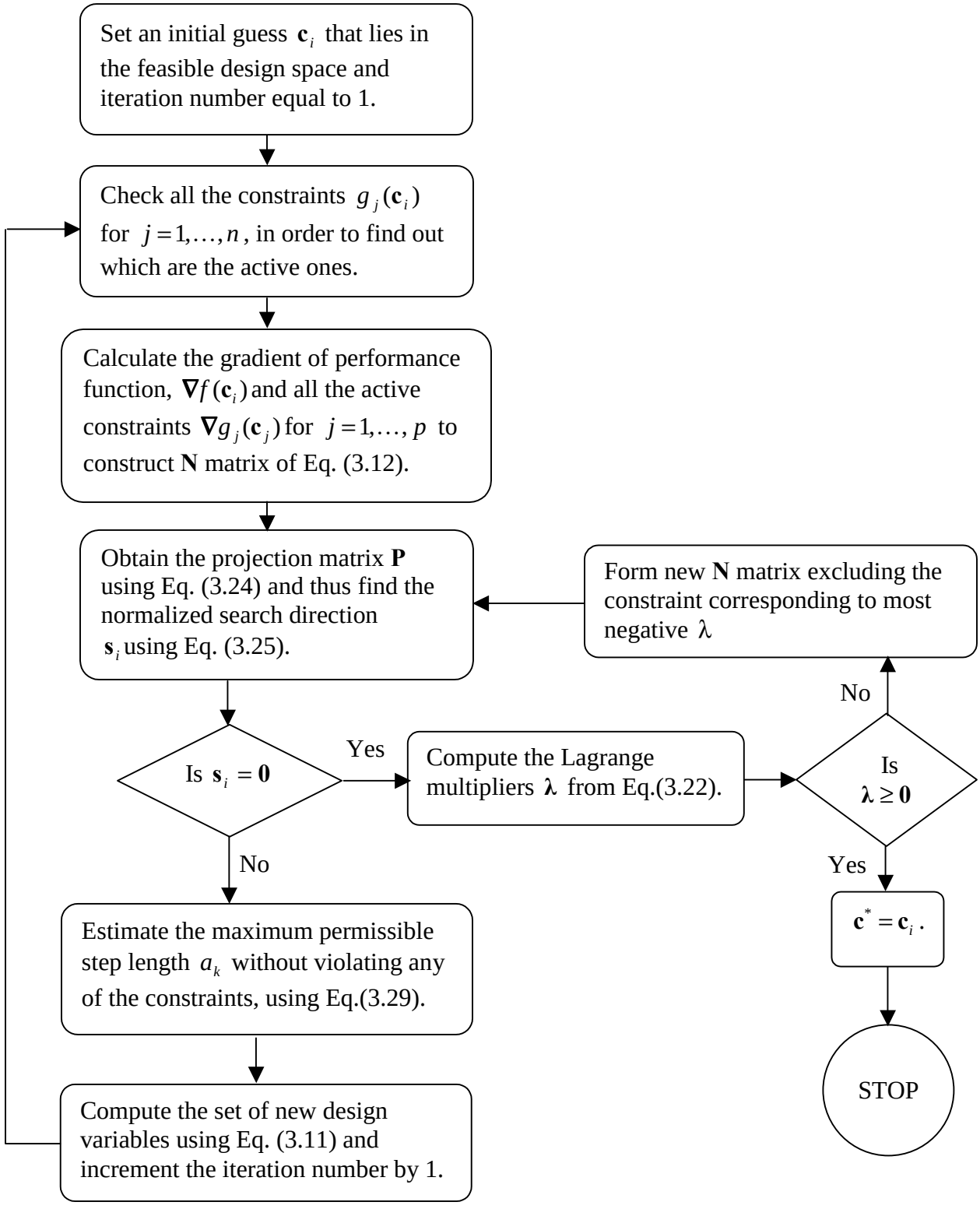

Figure 3.1: Flowchart Showing Steps of Rosen's Gradient Projection Technique.

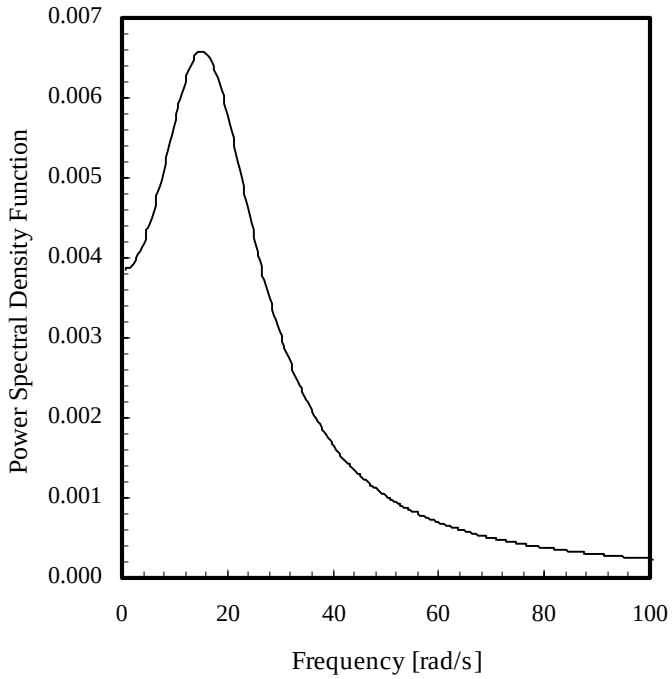

Figure 3.2: Power spectral density function of the Kanai-Tajimi form (ω_g = 18.85 rad/s, β_g = 0.65 and S = 0.0619 $m^2/s^3/rad$).

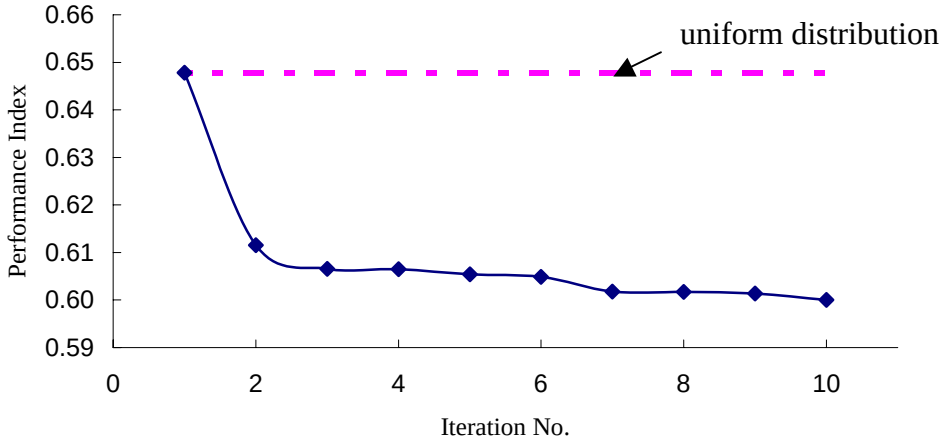

Figure 3.3: Evolution of Optimal Solution in Different Iterations for the Drift-based Performance index.

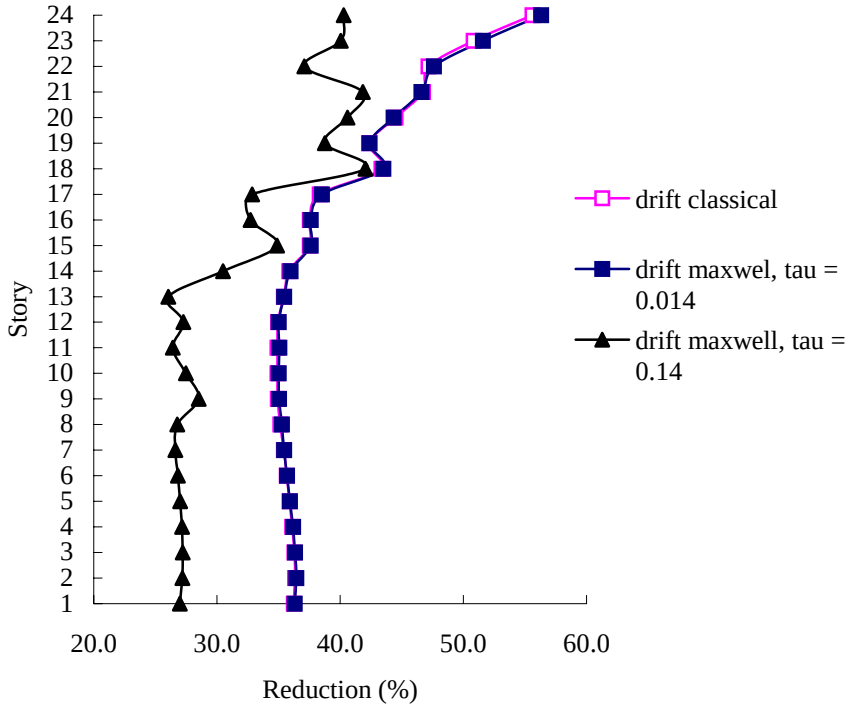

Figure 3.4: Comparision of Drift Response Reductions by Viscous and Maxwell Models for $\tau_d = 0.014$ and $\tau_d = 0.14$.

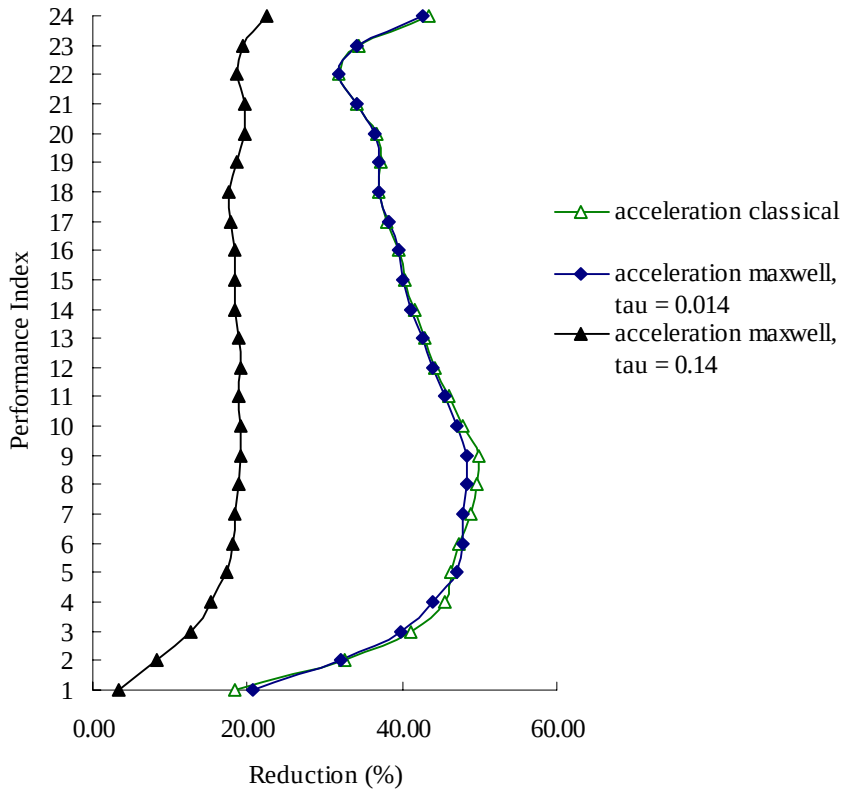

Figure 3.5: Comparision of Acceleration Response Reductions by Viscous and Maxwell Models for $\tau_d = 0.14$ and $\tau_d = 0.14$.

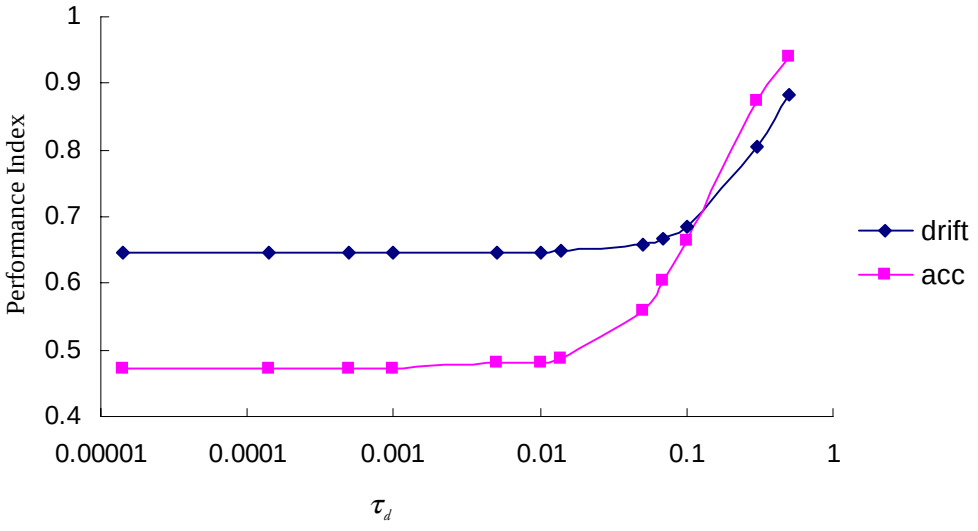

Figure 3.6: Effect of τ_d on Drift and Acceleration Performance Indices for Uniform Distribution of Total Damping.

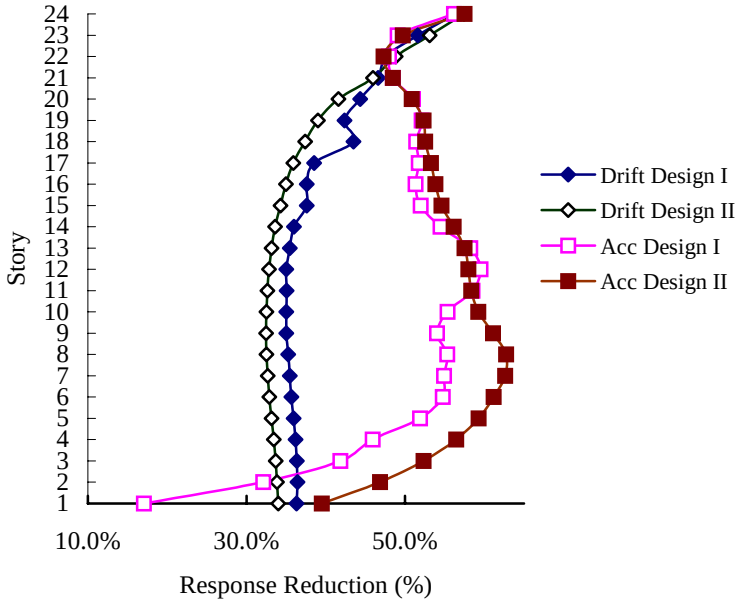

Figure 3.7: Cross-effectiveness of Acceleration-based and Drift-based Designs.

Chapter 4

Effect of Bracing Stiffness

4.1 Introduction

The damping devices are installed in a structure on braces to transmit the damping force. The development of the equations of motion in Chapter 2 and the formulation and solution of optimization problem in the previous chapter was based on the premise that the braces were perfectly rigid. The optimization problem then only considered the damping coefficient values of the damping device to be the design variables. In this chapter, we will investigate the effect of bracing flexibility. There are several bracing configuration that one can use, Figure 4.1. One can also utilize special braces to amplify the damping force using mechanical advantage. Constantinou and his colleagues (Constantinou *et al*., 1997) have proposed several configurations for this purpose. In this study, we will not be concerned with such special braces. Using such braces with mechanical advantage, one can use a smaller damper to provide the same damping force. Thus, their effect can be simply incorporated by a simple adjustment of the optimally calculated device parameters. In this chapter we will be primarily concerned with the investigation of the effect of brace flexibility on the damped system response. We will also examine if one can change the bracing stiffness to optimize the damper performance.

4.2 Equivalent Bracing Stiffness

For simplicity of presentation we will assume that the dampers are installed on Cheveron braces. Figure 4.2 shows such a brace with damping device in a building story. This figure is similar to Figure 2.4, except that now the brace is flexible with a spring coefficient of k_b. The effect of this brace flexibility in the equations of motion and in the formulation of the optimization problem can be included by replacing the damper

stiffness coefficient k_d with an equivalent stiffness coefficient k_e. Since the brace and the stiffness element of the damper are in series, this equivalent stiffness coefficient can be defined as:

$$k_e = \frac{k_d k_b}{k_d + k_b} \tag{4.1}$$

where k_b and k_d are the stiffness of bracing in a particular story and the device in that story, respectively. It is noted that the damper stiffness terms k_d only appear in the additional stiffness terms $\mathbf{K}_d$, $\mathbf{K}_d^*$ and $\mathbf{K}_d^{**}$ of Eq (2.4). Replacing k_d by equivalent stiffness coefficients of Eq. (4.1) new matrices are obtained. These changed matrices will be denoted by $\mathbf{K}_e$, $\mathbf{K}_e^*$ and $\mathbf{K}_e^{**}$.

The rigidity of the brace stiffness is expressed in terms of the stiffness ratio *SR* defined as follows:

$$SR = \frac{k_b}{k_s} \tag{4.2}$$

where k_b and k_s, respectively, are the stiffness coefficients of the brace and building story in which the brace is installed. To numerically examine the effect of bracing stiffness, an optimal damper distribution design with rigid bracing was considered. The bracing stiffness of this design was then gradually decreased, and the corresponding performance function values were calculated. In Figure 4.3 we plot the calculated performance function values for different stiffness ratios. It is noted that performance function value improves as the bracing stiffness values increase. It is mentioned that system was optimally designed for the rigid bracing case, and thus the optimality of the damping distribution is lost at the lower values of the stiffness ratio. From the figure, however, it is noted that the improvement in the performance is small for stiffness ratios higher that 5. Thus, the bracings with stiffness ratios more than 5 may be considered rigid.

Next it was examined to see if there are other optimal values between 0 and 5 for the stiffness ratios that will improve the performance. For this, the stiffness coefficients of the braces in each story were also considered independent design variables in the

optimization analysis. Thus, in addition to the variables of the damping coefficients, we now also have the bracing stiffness as the design variables, which can be varied to obtain the optimal performance.

While solving the optimization problem, some numerical problems were encountered because the values of the design variables of damping coefficients and stiffness coefficients were of different orders of magnitude. This required the use of a normalization procedure to remove these large differences. For this, the variables of the damping coefficient were normalized by 10% of the total damping coefficient value to be distributed. The design variable representing the bracing stiffness was expressed as the inverse of the stiffness ratio *SR* defined in Eq. (4.2). These two design variables are expressed as follows:

$$r_{d_i} = \frac{c_{d_i}}{0.1C_T} \tag{4.3}$$

$$r_{b_i} = \frac{k_{s_i}}{k_{b_i}} \tag{4.4}$$

For the stiffness ratio values varying between 0 and 5, the normalized design variable values are of the same order.

The modified optimization problem is now formulated as:

$$\text{Minimize } f[\mathbf{R}(\mathbf{r}_c, \mathbf{r}_b)] \tag{4.5}$$

subject to the following constraints:

$$\sum_{i=1}^{n} r_{c_i} - 10 = 0 \tag{4.6}$$

$$0.2 \le r_{b_i} \le 1 ; \quad i = 1,...,n \tag{4.7}$$

$$0 \le r_{c_i} \le 10 ; \quad i = 1,...,n \tag{4.8}$$

The associated Kuhn-Tucker conditions are

$$f_{,i}(\mathbf{c}^*) + \sum_{j \in A} \lambda_j = 0 \qquad i = 1,...,n \tag{4.9}$$

$$\sum_{i=1}^{n} r_{c_i} - 10 = 0 \tag{4.10}$$

$$r_{c_j} = 0 \qquad j \in A \tag{4.11}$$

$$r_{c_j} - 10 = 0 \qquad j \in A \tag{4.12}$$

$$r_{b_j} - 0.2 = 0 \qquad j \in A \tag{4.13}$$

$$r_{b_j} - 1.0 = 0 \qquad j \in A \tag{4.14}$$

The performance index is now a function of the two sets of design variables. To calculate the gradients of various response quantities with respect to these new variables we use the chain rule as follows. The derivatives of the matrices containing the damping coefficients with respect to the new design variables r_{c_i} are obtained as:

$$\frac{\partial \mathbf{C}}{\partial r_{c_i}} = \frac{\partial \mathbf{C}}{\partial c_{d_i}} \frac{\partial c_{d_i}}{\partial r_{c_i}} = 0.1 C_T \frac{\partial \mathbf{C}}{\partial c_{d_i}} \tag{4.15}$$

$$\frac{\partial \mathbf{C}}{\partial r_{b_i}} = 0 \tag{4.16}$$

Similarly the derivatives of the elements of supplementary stiffness matrices containing the equivalent bracing stiffness terms is obtained from the following formulas:

$$\frac{\partial \mathbf{K}}{\partial r_{c_i}} = \frac{\partial \mathbf{K}}{\partial k_{e_i}} \frac{\partial k_{e_i}}{\partial c_{d_i}} \frac{\partial c_{d_i}}{\partial r_{c_i}} = 0.1 C_T \frac{\gamma k_b^2}{(k_b + \gamma c_d)^2} \frac{\partial \mathbf{K}}{\partial k_{e_i}} \;;\; \gamma = \frac{k_d}{c_d} \tag{4.17}$$

$$\frac{\partial \mathbf{K}}{\partial r_{b_i}} = \frac{\partial \mathbf{K}}{\partial k_{e_i}} \frac{\partial k_{e_i}}{\partial k_{b_i}} \frac{\partial k_{b_i}}{\partial r_{b_i}} = \frac{-k_{s_i}}{r_{b_i}^2} \frac{\gamma^2 c_d^2}{(k_b + \gamma c_d)^2} \frac{\partial \mathbf{K}}{\partial k_{e_i}} = \frac{-k_{b_i}^2}{k_{s_i}} \frac{\gamma^2 c_d^2}{(k_b + \gamma c_d)^2} \frac{\partial \mathbf{K}}{\partial k_{e_i}} \tag{4.18}$$

Once, the gradients are known, the optimization problem is solved in the similar fashion, of course, now with increased set of variables.

4.3 Numerical Results

Several numerical results are obtained for the revised optimization problem for the same building structure. Tables 4.1 and 4.2 show the optimal values of the damping coefficients and story stiffness ratios obtained by minimizing the drift-based and base

shear-based performance indices, respectively. Both tables contain the results for relaxation time parameter values of 0.014 and 0.14. For all these results, the performance index is minimized keeping the total damping value equal to that of rigid bracing; the tables also contain the optimal damping coefficient values for the rigid bracing case. It is noted that the rigid bracing system provides the best performance measured in terms of the performance index values. It is noted that the optimal stiffness ratio values tend to move higher towards the upper limit of the bracing stiffness, especially in the stories with more significant damping coefficient values. This is because a rigid bracing enables the damper to be utilized more completely than a flexible bracing. The effectiveness of the damper with smaller relaxation time parameter values is also higher for the same reason; the smaller time relaxation parameter values corresponds to a stiffer spring element in parallel with the damper element in the Maxwell model. It is also noted that the reduction in some response quantities may be more sensitive to the changes in the time relaxation parameter than others. For example, reduction in the base shear affected more by the time relaxation parameter than the story drifts.

In Figures 4.4, and 4.5 we plot the response reductions along the building height corresponding to the designs presented in Tables 4.1, 4.2, respectively. The values corresponding to the rigid bracing cases are also plotted. In Figure 4.4 is shown the percent reduction for the story drifts for the story drift-based performance index. In Figure 4.5 we show the percent reduction in the story shear for the base-shear based performance index. It is noted that the rigid braces provide the best reduction in story responses in all cases.

4.4 Chapter Summary

In this chapter, we have examined the effect of bracing flexibility on the effectiveness of the Maxwell dampers. We also examined the possibility of optimizing the bracing stiffness in various stories; for this, the optimization problem was re-formulated to include the stiffness of braces in different stories as new design variables. It was observed that increasing the rigidity of bracing increased the effectiveness of dampers. The optimal search also tended to force the bracing stiffness toward its upper limit set in the

optimization procedure. A brace with stiffness about five times the story stiffness can be considered to be practically rigid.

Table 4.1: Numerical Results for Drift Based Response for total damping

$C_T = 1.32 \times 10^9$

Story Mode	***Flexible Bracing***				***Rigid***
	$\tau_d = 0.14$		$\tau_d = 0.014$		
	SR	c_d^* ***[% of*** C_T ***]***	***SR***	c_d^* ***[% of*** C_T ***]***	c_d^* ***[% of*** C_T ***]***
1	0.00	0.00	0.000	0.00	0.00
2	0.00	0.00	0.000	0.00	0.00
3	0.00	0.00	0.000	0.00	0.00
4	0.00	0.00	0.000	0.00	0.00
5	0.00	0.00	0.000	0.00	0.00
6	0.00	0.00	0.000	0.00	0.00
7	0.00	0.00	0.000	0.00	0.00
8	2.36	1.51	0.000	0.00	1.06
9	5.00	6.35	3.469	7.79	6.24
10	3.09	4.14	2.444	4.71	3.97
11	2.42	1.79	2.135	1.34	1.43
12	3.05	3.72	2.649	4.63	3.60
13	2.33	0.95	0.000	0.00	0.00
14	5.00	8.22	5.000	8.93	8.33
15	5.00	11.05	5.000	12.80	13.64
16	5.00	8.22	5.000	8.79	8.50
17	5.00	7.14	5.000	7.49	7.06
18	5.00	11.37	5.000	12.45	16.26
19	5.00	8.30	5.000	8.83	10.36
20	5.00	8.11	5.000	8.14	8.87
21	5.00	7.86	5.000	7.34	6.94
22	5.00	4.80	5.000	3.69	2.02
23	5.00	4.73	5.000	3.09	1.74
24	5.00	1.74	0.000	0.00	0.00
$f(\mathbf{c}^*)$	0.6729		0.6022		0.6000
Reduction [%]	32.71		39.77		40.00

Table 4.2: Numerical Results for Base Shear for total damping $C_T = 3.88\times10^8$

Story Mode	***Flexible Bracing***				***Rigid***
	$\tau_d = 0.14$		$\tau_d = 0.014$		
	SR	c_d^* ***[% of*** C_T ***]***	***SR***	c_d^* ***[% of*** C_T ***]***	c_d^* ***[% of*** C_T ***]***
1	0.00	0.00	0.00	0.00	0.00
2	0.00	0.00	0.00	0.00	0.00
3	0.00	0.00	0.00	0.00	0.00
4	0.00	0.00	0.00	0.00	0.00
5	0.00	0.00	0.00	0.00	0.00
6	0.00	0.00	0.00	0.00	0.00
7	0.00	0.00	0.00	0.00	0.00
8	0.00	0.00	0.00	0.00	1.63
9	0.00	0.00	2.03	0.44	2.49
10	0.00	0.00	2.04	1.40	2.32
11	0.00	0.00	2.04	0.44	2.12
12	0.00	0.00	0.00	0.00	3.23
13	0.00	0.00	0.00	0.00	1.95
14	2.06	2.40	1.99	2.93	3.25
15	2.14	5.20	1.98	4.73	5.32
16	2.12	4.23	2.03	5.32	6.50
17	2.17	4.24	2.34	4.95	5.05
18	3.04	10.13	1.72	7.79	6.46
19	2.81	8.49	2.34	8.88	9.07
20	5.00	11.39	3.60	12.55	9.56
21	5.00	15.08	5.00	15.88	11.68
22	5.00	13.40	5.00	14.40	13.24
23	5.00	15.11	5.00	13.29	9.93
24	5.00	10.33	5.00	7.01	6.18
$f(\mathbf{c}^*)$	0.8132		0.6119		0.6021
Reduction [%]	18.68		38.81		39.79

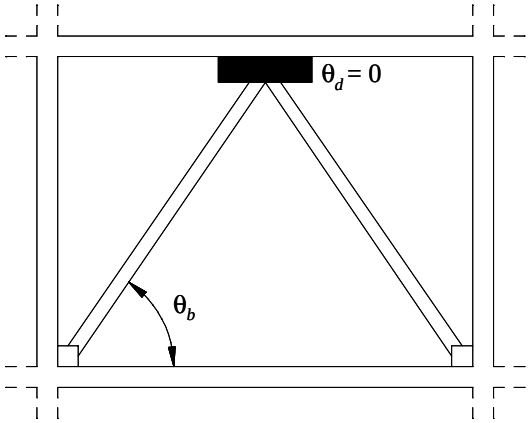

(a)

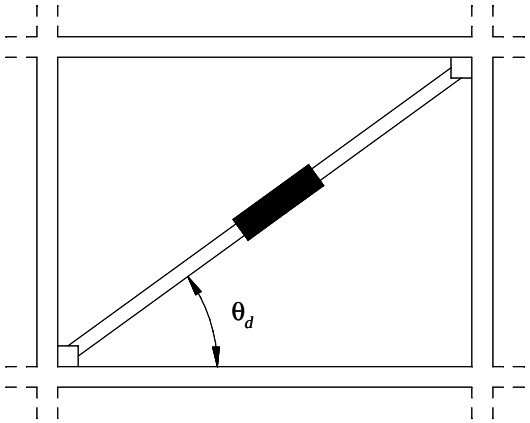

(b)

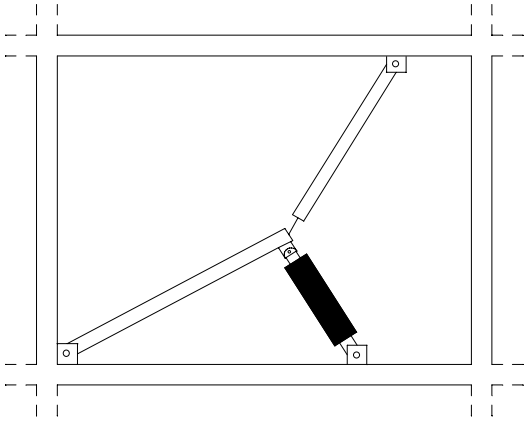

(c)

Figure 4.1: Typical configurations of damping devices and bracings, (a) chevron brace, (b) diagonal bracing, (c) toggle brace-damper system.

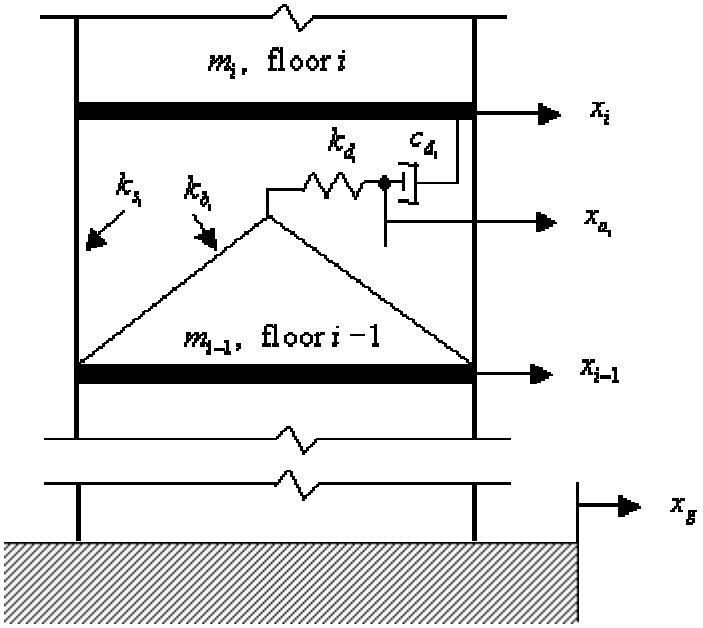

Figure 4.2: A Bay with Flexible Chevron Bracing for Floor *i*.

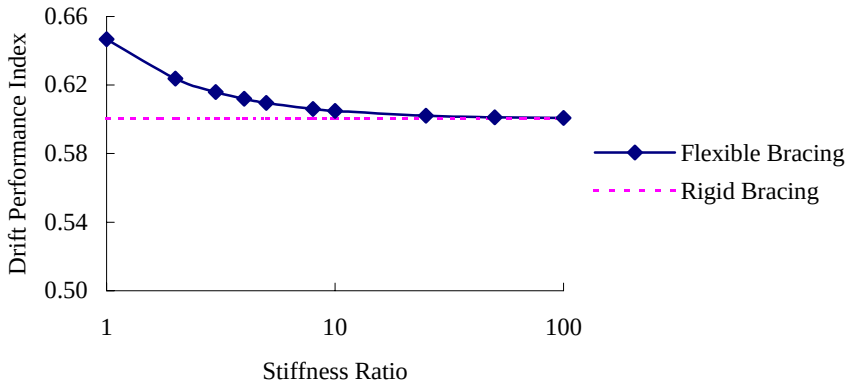

Figure 4.3: Variation of Drift Based Performance Index with Stiffness Ratio.

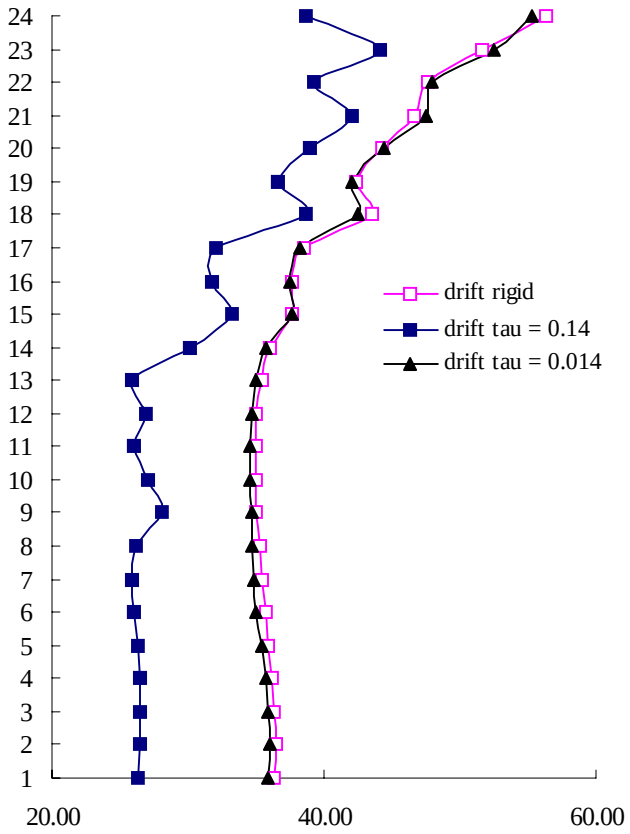

Figure 4.4: Comparision of Reduction in Drift Responses for Rigid and Flexible Bracings.

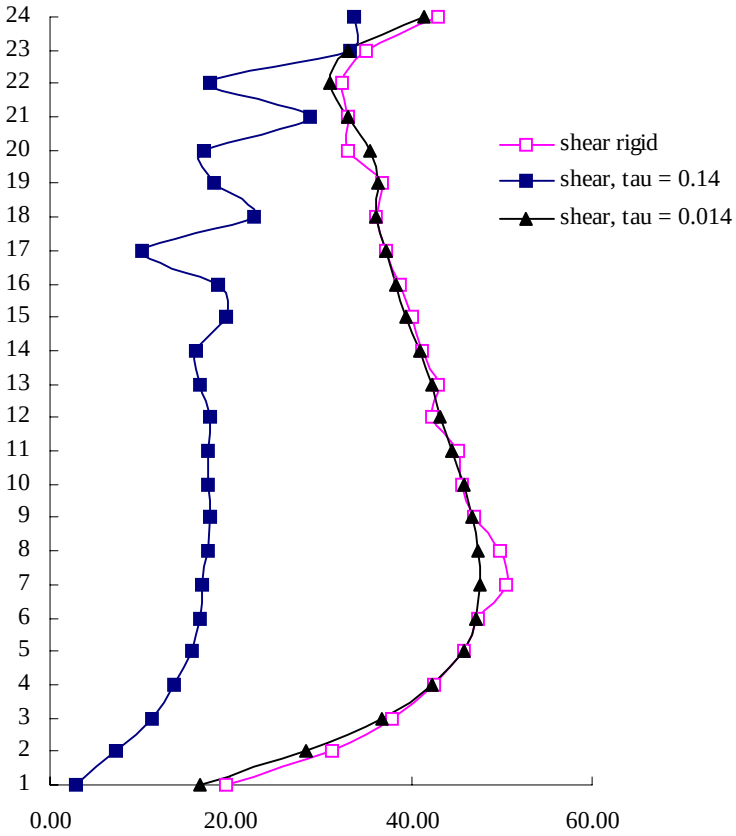

Figure 4.5: Comparision of Reduction in Base Shear Responses for Rigid and Flexible Bracings.

Chapter 5

Summary and Concluding Remarks

5.1 Summary

This study has focused on the optimal usage of fluid visco-elastic devices for optimal response control of building structures subjected to earthquake induced ground motions. The applicability of such energy dissipation devices in passive control of structures is quite well known. Herein we explore the optimal usage of these devices, especially those that need to be modeled by the Maxwell model of visco-elastic materials.

Chapter 2 gives a brief discussion of different models that have been used or considered appropriate to represent the visco-elastic dampers. Although classical velocity dependent force models are widely used to represent fluid dampers, they have their own limitations. Some fluid dampers exhibit frequency dependence in their force-deformation relationships, especially the stiffening effect at higher frequencies of deformation. For such dampers, models with different spring and dashpot combinations have been proposed in the literature. One such model that has been considered for such behavior is the Maxwell model. As mentioned before, the focus of the analytical development in Chapter 2 is on this particular model. The equations of motion developed earlier for structures with Maxwell dampers were non-symmetric and thereby making associated eigen-value problem non self-adjoint. Using the Lagrange equations, the symmetric self-adjoint system of equations have been developed in Chapter 2. Using these equations of motion, a symmetric set of first order state space equations are defined. They are then solved to define a response quantity by the modal analysis approach.

Chapter 3 formulates the optimization problem for the calculation of optimal design parameters of dampers. An objective function for optimization problem is defined in terms of a performance index representing the normalized response of the structure.

The responses considered in the study are the story drifts, floor accelerations and base shear. Rosen's gradient projection technique is chosen to search for the optimal solution. The formulas needed to calculate the gradient of objective function and other associated quantities are presented. In the end, several sets of numerical results are presented for a 24-story shear building structure. The optimal values of the design variables of device damping coefficients are obtained for the drift-based, acceleration-based, and base shear-based performance indices. Procedure is established to calculate the optimal values of the design variables for achieving a desired reduction in the performance index. Parametric study is conducted to examine the effect of relaxation time parameter of the model. In Chapter 3, the braces employed to install the damping devices in the structure were considered rigid. In Chapter 4, however, the effect of brace flexibility on the effectiveness of dampers is investigated. The possibility of optimizing the brace stiffness coefficients is also explored by redefining the optimization problem with these stiffness coefficients as additional design variables.

5.2 Conclusions

Specific conclusions drawn in this study, based on the numerical example, are described in different chapters where numerical results are presented. In the following, we only present the broader conclusion of this study.

1. It is shown that by using a symmetric formulation of the equations of motion, the procedure for response analysis and for optimal search by a gradient-based scheme can be significantly simplified, especially if modal analysis procedure is desired. It is primarily because a symmetric system only needs one set of eigenproperties.
2. It is observed that ignoring the stiffening effect in viscous fluid dampers if this effect is, indeed, present can lead to an unconservative design with these dampers. This is illustrated by comparing the response reducing effect of a Maxwell damper with that of a classical damper with equal damping coefficient. For the same value of damping coefficient, the response reduction is smaller if the damper is modeled as a Maxwell damper than if it is modeled as a classical damper which ignores the stiffening effect at higher deformation frequencies.

This effect is more pronounced if the relaxation time parameter of the Maxwell model is large.

3. The more rigid the bracing the better the damper effectiveness. Since a brace cannot be made perfectly rigid, a brace with stiffness coefficient 5.0 times as large as the stiffness coefficient of the building story in which the brace is installed will provide adequate rigidity.

Appendix

A. Partial Fraction Coefficients

The partial fraction coefficients required in Eqs. (2.48) and (2.49) are defined as (Moreschi, 2000):

$$W_{lijk} = -\left\{\left(\Omega^2 - \Omega^{-2}\right)\mu_{lijk} - 2\left[1 - \Omega^2 + 2\left(\beta_j^2\,\Omega^2 - \beta_k^2\right)\right]\eta_{lijk}\right\}/\,\delta_{jk} \tag{A.1}$$

$$Q_{lijk} = \left\{\left(\Omega^2 - \Omega^{-2}\right)\eta_{lijk} - 2\,\Omega^{-2}\left[1 - \Omega^2 + 2\left(\beta_k^2\,\Omega^2 - \beta_j^2\right)\mu_{lijk}\right]\right\}/\left(\omega_j^2\,\delta_{jk}\right) \tag{A.2}$$

$$A_{lijk} = \alpha_j\left(-\{\mathbf{g}_{li}\}_k + 2\,\{\mathbf{a}_{li}\}_k\,\alpha_j\right)/\,\gamma_{jk} \tag{A.3}$$

$$B_{lijk} = -\omega_k^2\left[2\{\mathbf{a}_{li}\}_k\,\omega_k^2 + \{\mathbf{g}_{li}\}_k\left(\alpha_j + 2\,\omega_k\,\beta_k\right)\right]/\,\gamma_{jk} \tag{A.4}$$

$$C_{lijk} = \left[\{\mathbf{g}_{li}\}_k\,\alpha_j + 2\{\mathbf{a}_{li}\}_k\,\omega_k\left(\omega_k + 2\,\alpha_j\,\beta_k\right)\right]/\,\gamma_{jk} \tag{A.5}$$

with

$$\Omega = \omega_j\,/\,\omega_k \tag{A.6}$$

$$\begin{aligned}\eta_{lijk} = {} & \{\mathbf{g}_{li}\}_j\{\mathbf{g}_{li}\}_k\left(1 - 4\,\beta_j^2 + 4\,\beta_j\,\beta_k\,\Omega - \Omega^2\right) + \\ & 4\,\omega_j^2\{\mathbf{a}_{li}\}_j\{\mathbf{a}_{li}\}_k\left(1 - \Omega^2\right) + 4\,\omega_j\left(\{\mathbf{a}_{li}\}_j\{\mathbf{g}_{li}\}_k - \{\mathbf{a}_{li}\}_k\{\mathbf{g}_{li}\}_j\right)\left(\beta_k\,\Omega - \beta_j\right)\end{aligned} \tag{A.7}$$

$$\begin{aligned}\mu_{lijk} = {} & \{\mathbf{g}_{li}\}_j\{\mathbf{g}_{li}\}_k\left(\Omega^2 - 1\right) + 4\,\omega_j^2\{\mathbf{a}_{li}\}_j\{\mathbf{a}_{li}\}_k\left[\left(1 - 4\,\beta_j^2\right)\Omega^2 + 4\,\beta_j\,\beta_k\,\Omega - 1\right] + \\ & 4\,\omega_j\,\Omega\left(\{\mathbf{a}_{li}\}_j\{\mathbf{g}_{li}\}_k - \{\mathbf{a}_{li}\}_k\{\mathbf{g}_{li}\}_j\right)\left(\beta_j\,\Omega - \beta_k\right)\end{aligned} \tag{A.8}$$

$$\delta_{jk} = 16\left(\beta_j^2 + \beta_k^2 - \beta_j^4 - \beta_k^4\right) + 4\left(\Omega^2 + \Omega^{-2}\right)\left[1 - 2\left(\beta_j^2 + \beta_k^2 - 2\,\beta_j^2\,\beta_k^2\right)\right] - \Omega^{-4} - \Omega^4 - 6 \tag{A.9}$$

$$\gamma_{jk} = \omega_k^2 + \alpha_j^2 + 2\,\alpha_j\,\omega_k\,\beta_k \tag{A.10}$$

B. Derivatives of Eigenproperties

Equation of Motion

$$\mathbf{A}_s \dot{\mathbf{z}}(t) + \mathbf{B}_s \mathbf{z}(t) = -\mathbf{D}_s \begin{Bmatrix} \mathbf{E} \\ \mathbf{0} \\ \mathbf{0} \end{Bmatrix} \ddot{X}_g(t) \tag{B.1}$$

$$\mathbf{A} = \begin{bmatrix} \mathbf{0} & \mathbf{0} & \mathbf{M}_s \\ \mathbf{0} & \mathbf{C}_d^* & -\mathbf{C}_d \\ \mathbf{M}_s & -\mathbf{C}_d^T & \mathbf{C}_s + \mathbf{C}_d^{**} \end{bmatrix};\ \mathbf{B} = \begin{bmatrix} -\mathbf{M}_s & \mathbf{0} & \mathbf{0} \\ \mathbf{0} & \mathbf{K}_d^* & -\mathbf{K}_d \\ \mathbf{0} & -\mathbf{K}_d^T & \mathbf{K}_s + \mathbf{K}_d^{**} \end{bmatrix}; \tag{B.2}$$

Derivatives of Eigenvalues

Eigenvalue Problem is defined as

$$-\mu_j \mathbf{A}\{\phi\}_j = \mathbf{B}\{\phi\}_j \tag{B.3}$$

or

$$\mathbf{B}\{\phi\}_j + \mu_j \mathbf{A}\{\phi\}_j = 0 \tag{B.4}$$

or

$$\mathbf{F}_j\{\phi\}_j = 0 \quad \text{where } \mathbf{F}_j = \mu_j \mathbf{A} + \mathbf{B} \tag{B.5}$$

Pre-multiplying by $\{\phi\}_j^T$

$$\{\phi\}_j^T \mathbf{F}_j \{\phi\}_j = 0 \tag{B.6}$$

Taking derivative w.r.t. *c*,

$$\frac{\partial \{\phi\}_j^T}{\partial c} \mathbf{F}_j \{\phi\}_j + \{\phi\}_j^T \frac{\partial \mathbf{F}_j}{\partial c} \{\phi\}_j + \{\phi\}_j^T \mathbf{F}_j \frac{\partial \{\phi\}_j}{\partial c} = 0 \tag{B.7}$$

The first and third term in Eq. (B.7) being symmetric, Eq. (B.7) may be written as:

$$2\frac{\partial \{\phi\}_j^T}{\partial c} \mathbf{F}_j \{\phi\}_j + \{\phi\}_j^T \frac{\partial \mathbf{F}_j}{\partial c} \{\phi\}_j = 0 \tag{B.8}$$

Using Eq. (B.5), Eq. (B.8) yields

$$\{\phi\}_j^T \frac{\partial \mathbf{F}_j}{\partial c} \{\phi\}_j = 0 \tag{B.9}$$

$$\Rightarrow \qquad \{\phi\}_j^T \frac{\partial[\mu_j \mathbf{A} + \mathbf{B}]}{\partial c}\{\phi\}_j = 0 \tag{B.10}$$

$$\{\phi\}_j^T \frac{\partial \mu_j}{\partial c}\mathbf{A}\{\phi\}_j + \{\phi\}_j^T \mu_j \frac{\partial \mathbf{A}}{\partial c}\{\phi\}_j + \{\phi\}_j^T \frac{\partial \mathbf{B}}{\partial c}\{\phi\}_j = 0 \tag{B.11}$$

$$\frac{\partial \mu_j}{\partial c} = -\frac{\{\phi\}_j^T \left[\mu_j \frac{\partial \mathbf{A}}{\partial c} + \frac{\partial \mathbf{B}}{\partial c}\right]\{\phi\}_j}{\{\phi\}_j^T \mathbf{A}\{\phi\}_j} \tag{B.12}$$

If the eigenvectors are orthonormalized w.r.t. $\mathbf{A}$, such that

$$\{\phi\}_i^T \mathbf{A}\{\phi\}_j = \delta_{ij} \tag{B.13}$$

Then

$$\{\phi\}_j^T \mathbf{B}\{\phi\}_j + \mu_j \{\phi\}_j^T \mathbf{A}\{\phi\}_j = 0 \tag{B.14}$$

$$\{\phi\}_j^T \mathbf{B}\{\phi\}_j = -\mu_j \tag{B.15}$$

Thus,

$$\frac{\partial \mu_j}{\partial c} = -\{\phi\}_j^T \left[\mu_j \frac{\partial \mathbf{A}}{\partial c} + \frac{\partial \mathbf{B}}{\partial c}\right]\{\phi\}_j \tag{B.16}$$

Now,

$$\frac{\partial \mathbf{A}}{\partial c} = \begin{bmatrix} \mathbf{0} & \mathbf{0} & \mathbf{0} \\ \mathbf{0} & \frac{\partial \mathbf{C}_d}{\partial c} & -\frac{\partial \mathbf{C}_d}{\partial c} \\ \mathbf{0} & -\frac{\partial \mathbf{C}_d}{\partial c} & \frac{\partial \mathbf{C}_d}{\partial c} \end{bmatrix} = \begin{bmatrix} \mathbf{0} & \mathbf{0} \\ \mathbf{0} & \frac{\partial \mathbf{C}}{\partial c} \end{bmatrix}; \; \frac{\partial \mathbf{B}}{\partial c} = \begin{bmatrix} \mathbf{0} & \mathbf{0} & \mathbf{0} \\ \mathbf{0} & \frac{\partial \mathbf{K}_d^*}{\partial c} & -\frac{\partial \mathbf{K}_d}{\partial c} \\ \mathbf{0} & -\frac{\partial \mathbf{K}_d^T}{\partial c} & \frac{\partial \mathbf{K}_d^{**}}{\partial c} \end{bmatrix} = \begin{bmatrix} \mathbf{0} & \mathbf{0} \\ \mathbf{0} & \frac{\partial \mathbf{K}}{\partial c} \end{bmatrix} \tag{B.17}$$

where

$$\mathbf{C} = \begin{bmatrix} \mathbf{C}_d^* & -\mathbf{C}_d \\ -\mathbf{C}_d^T & \mathbf{C}_s + \mathbf{C}_d^{**} \end{bmatrix}; \; \mathbf{K} = \begin{bmatrix} \mathbf{K}_d^* & -\mathbf{K}_d \\ -\mathbf{K}_d^T & \mathbf{K}_s + \mathbf{K}_d^{**} \end{bmatrix} \tag{B.18}$$

Hence,

$$\mu_{j_i} = -\{\phi^L\}_j^T (\mu_j \mathbf{C}_{,i} + \mathbf{K}_{,i})\{\phi^L\}_j \tag{B.19}$$

where $\{\phi^L\}_j$ is part of $\{\phi\}_j$ containing lower $n_a + n$ elements.

Derivatives of Eigenvectors

Expansion theorem says

$$\frac{\partial\{\phi\}_j}{\partial c} = \sum_{l=1}^{2n+n_a} a_{jl}\{\phi\}_l \tag{B.20}$$

From Eq. (B.5)

$$\mathbf{F}_j\{\phi\}_j = \mathbf{0} \tag{B.21}$$

Taking derivatives on both sides w.r.t. c

$$\frac{\partial\mathbf{F}_j}{\partial c}\{\phi\}_j + \mathbf{F}_j\frac{\partial\{\phi\}_j}{\partial c} = \mathbf{0} \tag{B.22}$$

Using Eq. (B.20)

$$\mathbf{F}_j\sum_{l=1}^{2n+n_a} a_{jl}\{\phi\}_l = -\frac{\partial\mathbf{F}_j}{\partial c}\{\phi\}_j \tag{B.23}$$

Pre-multiplying by $\{\phi\}_k^T$,

$$\sum_{l=1}^{2n+n_a} a_{jl}\{\phi\}_k^T\mathbf{F}_j\{\phi\}_l = -\{\phi\}_k^T\frac{\partial\mathbf{F}_j}{\partial c}\{\phi\}_j \tag{B.24}$$

Substituting Eq. (B.5) into Eq. (B.24)

$$\sum_{l=1}^{2n+n_a} a_{jl}\{\phi\}_k^T[\mu_j\mathbf{A}+\mathbf{B}]\{\phi\}_l = -\{\phi\}_k^T\frac{\partial\mathbf{F}_j}{\partial c}\{\phi\}_j \tag{B.25}$$

Using Eqs. (B.13) and (B.15)

$$\sum_{l=1}^{2n+n_a} a_{jl}[\mu_j\delta_{kl} - \mu_l\delta_{kl}] = -\{\phi\}_k^T\frac{\partial\mathbf{F}_j}{\partial c}\{\phi\}_j \tag{B.26}$$

If $k = l$,

$$a_{jl}[\mu_j - \mu_l]\{\phi\}_l = -\{\phi\}_l^T\frac{\partial\mathbf{F}_j}{\partial c}\{\phi\}_j \tag{B.27}$$

$$a_{jl} = -\frac{\{\phi\}_l^T\dfrac{\partial\mathbf{F}_j}{\partial c}\{\phi\}_j}{(\mu_l - \mu_j)} \tag{B.28}$$

Equations (B.5), (B.16) to (B.18) give

$$a_{jl} = -\frac{\{\phi\}_l^T \left[\mu_j \frac{\partial \mathbf{A}}{\partial c} + \frac{\partial \mathbf{B}}{\partial c}\right]\{\phi\}_j}{(\mu_l - \mu_j)} \tag{B.29}$$

$$a_{jl} = -\frac{\{\phi^L\}_l^T \left[\mu_j \frac{\partial \mathbf{C}}{\partial c} + \frac{\partial \mathbf{K}}{\partial c}\right]\{\phi^L\}_j}{(\mu_l - \mu_j)} = -\frac{1}{(\mu_l - \mu_j)}\left[\{\phi^L\}_l^T (\mu_j \mathbf{C}_{,i} + \mathbf{K}_{,i})\{\phi^L\}_j\right] \tag{B.30}$$

To obtain a_{jj},

$$\{\phi\}_j^T \mathbf{A}\{\phi\}_j = 1 \tag{B.31}$$

Taking derivatives on both sides of Eq. (B.31)

$$2\frac{\partial \{\phi\}_j^T}{\partial c}\mathbf{A}\{\phi\}_j + \{\phi\}_j^T \frac{\partial \mathbf{A}}{\partial c}\{\phi\}_j = 0 \tag{B.32}$$

Using Eq. (B.20),

$$2\sum_{l=1}^{2n+n_a} a_{jl}\{\phi\}_l^T \mathbf{A}\{\phi\}_j + \{\phi\}_j^T \frac{\partial \mathbf{A}}{\partial c}\{\phi\}_j = 0 \tag{B.33}$$

$$2\sum_{l=1}^{2n+n_a} a_{jl}\delta_{lj} + \{\phi\}_j^T \frac{\partial \mathbf{A}}{\partial c}\{\phi\}_j = 0 \tag{B.34}$$

$$a_{jj} = -\frac{1}{2}\{\phi\}_j^T \frac{\partial \mathbf{A}}{\partial c}\{\phi\}_j \tag{B.35}$$

Simplifying using Eq. (B.17)

$$a_{jj} = -\frac{1}{2}\{\phi^L\}_j^T \mathbf{C}_{,i}\{\phi^L\}_j \tag{B.36}$$

C. Gradients Calculations Formulas

In this section, the partial derivative formulas needed to calculate the gradients in Eq. (3.38) are provided (Moreschi, 2000). They are obtained by direct application of the chain rule of differentiation. Here, they are presented in compact forms, suitable for programming.

By denoting with $\nabla(\ )$ the row vector gradient of a given quantity and considering the scalar product of vectors, the derivatives of the response components $\boldsymbol{S}_{1i}$, $\boldsymbol{S}_{2i}$ and $\boldsymbol{S}_{3i}$

with respect to the d^{th} design variable are obtained from the chain rule of differentiation as:

$$\mathbf{S}_{1i,d} = \nabla \mathbf{S}_{1i} \cdot \left[\left\{ \mathbf{e}_{li} \right\}_{j,d}, \left\{ \mathbf{e}_{li} \right\}_{k,d}, \alpha_{j,d}, \alpha_{k,d}, J_{lj,d}, J_{lk,d} \right]^T \tag{C.1}$$

$$\mathbf{S}_{2i,d} = \nabla \mathbf{S}_{2i} \cdot \left[\left\{ \mathbf{e}_{li} \right\}_{j,d}, A_{lijk,d}, B_{lijk,d}, C_{lijk,d}, J_{lj,d}, I_{1lk,d}, I_{2lk,d} \right]^T \tag{C.2}$$

$$\mathbf{S}_{3i,d} = \nabla \mathbf{S}_{3i} \cdot \left[\left\{ \mathbf{g}_{li} \right\}_{j,d}, \left\{ \mathbf{g}_{li} \right\}_{k,d}, \left\{ \mathbf{a}_{li} \right\}_{j,d}, \left\{ \mathbf{a}_{li} \right\}_{k,d}, \Omega_{,d}, Q_{lijk,d}, W_{lijk,d}, I_{1lj,d}, I_{1lk,d}, I_{2lj,d}, I_{2lk,d} \right]^T \tag{C.3}$$

where

$$A_{lijk,d} = \nabla A_{lijk} \cdot \left[\alpha_{j,d}, \left\{ \mathbf{g}_{li} \right\}_{k,d}, \left\{ \mathbf{a}_{li} \right\}_{k,d}, \omega_{k,d}, \beta_{k,d} \right]^T \tag{C.4}$$

$$B_{lijk,d} = \nabla B_{lijk} \cdot \left[\alpha_{j,d}, \left\{ \mathbf{g}_{li} \right\}_{k,d}, \left\{ \mathbf{a}_{li} \right\}_{k,d}, \omega_{k,d}, \beta_{k,d} \right]^T \tag{C.5}$$

$$C_{lijk,d} = \nabla C_{lijk} \cdot \left[\alpha_{j,d}, \left\{ \mathbf{g}_{li} \right\}_{k,d}, \left\{ \mathbf{a}_{li} \right\}_{k,d}, \omega_{k,d}, \beta_{k,d} \right]^T \tag{C.6}$$

$$Q_{lijk,d} = \nabla Q_{lijk} \cdot \left[\left\{ \mathbf{g}_{li} \right\}_{j,d}, \left\{ \mathbf{g}_{li} \right\}_{k,d}, \left\{ \mathbf{a}_{li} \right\}_{j,d}, \left\{ \mathbf{a}_{li} \right\}_{k,d}, \Omega_{,d}, \omega_{j,d}, \beta_{j,d}, \beta_{k,d} \right]^T \tag{C.7}$$

$$W_{lijk,d} = \nabla W_{lijk} \cdot \left[\left\{ \mathbf{g}_{li} \right\}_{j,d}, \left\{ \mathbf{g}_{li} \right\}_{k,d}, \left\{ \mathbf{a}_{li} \right\}_{j,d}, \left\{ \mathbf{a}_{li} \right\}_{k,d}, \Omega_{,d}, \omega_{j,d}, \beta_{j,d}, \beta_{k,d} \right]^T \tag{C.8}$$

$$J_{lj,d} = \nabla J_{lj} \cdot \left[\omega_{j,d}, \beta_{j,d} \right]^T; \quad I_{1lj,d} = \nabla I_{1lj} \cdot \left[\omega_{j,d}, \beta_{j,d} \right]^T; \quad I_{2lj,d} = \nabla I_{2lj} \cdot \left[\omega_{j,d}, \beta_{j,d} \right]^T \tag{C.9}$$

$$\left\{ \mathbf{g}_{li} \right\}_{j,d} = \nabla \left\{ \mathbf{g}_{li} \right\}_{j} \cdot \left[\left\{ \mathbf{a}_{li} \right\}_{j,d}, \left\{ \mathbf{b}_{li} \right\}_{j,d}, \omega_{j,d}, \beta_{j,d} \right]^T \tag{C.10}$$

$$\left\{ \mathbf{a}_{li} \right\}_{j,d} = \mathrm{Re}\left[\left\{ \mathbf{q}_{li} \right\}_{j,d} \right]; \qquad \left\{ \mathbf{b}_{li} \right\}_{j,d} = \mathrm{Im}\left[\left\{ \mathbf{q}_{li} \right\}_{j,d} \right] \tag{C.11}$$

$$\Omega_{,d} = \frac{\left(\omega_k \, \omega_{j,d} - \omega_j \, \omega_{k,d} \right)}{\omega_k^2} \tag{C.12}$$

Finally, the derivatives of the performance indexes given by Eqs. (3.80) and (3.81) can be calculated as

$$\left[f_1(\mathbf{d}) \right]_{,d} = \frac{\left\{ E\left[\mathbf{R}_i(\mathbf{d}, t) \right] \right\}_{,d}}{E\left[R_{oi} \right]}, \qquad d = 1, \ldots, n_l \tag{C.13}$$

$$\left[f_2(\mathbf{d}) \right]_{,d} = \frac{\left\{ E\left[\mathbf{R}(\mathbf{d},t) \right] \right\} \cdot \left\{ E\left[\mathbf{R}(\mathbf{d},t) \right] \right\}_{,d}}{\left\| E\left[\mathbf{R}_o \right] \right\| \left\| E\left[\mathbf{R}(\mathbf{d},t) \right] \right\|}, \qquad d = 1,\ldots,n_l \tag{C.14}$$

References

1. Constantinou, M. C. and Symans, M. D., (1992). "Experimental and Analytical Investigation of Seismic Response of Structures with Supplemental Fluid Dampers," *Report No. NCEER 92-0032*, National Center for Earthquake Engineering Research, University of New York at Buffalo, Buffalo, NY.
2. Constantinou, M. C. and Symans, M. D., (1993). "Seismic Response of Structures with Supplemental Damping," *The Structural Design of Tall Buildings*, 2, 77-92.
3. Constantinou, M. C., Soong, T. T., and Dargush, G. F., (1998). *Passive Energy Dissipation Systems for Structural Design and Retrofit*, Monograph No. 1, Multidisciplinary Center for Earthquake Engineering Research, Buffalo, NY.
4. Constantinou, M. C., Tsopelas, P., and Hammel, W., (1997). "Testing and Modeling of an Improved Damper Configuration for Stiff Structural Systems," Technical Report submitted to the Center for Industrial Effectiveness and Taylor Devices, Inc.
5. Fox, R. L. and Kapoor, M. P., (1968). "Rates of Change of Eigenvalues and Eigenvectors," *AIAA Journal*, 6(12), 2426.
6. Ghafory-Ashtiany, M. and Singh, M. P., (1981). "Seismic Response of Structural System with Random Parameters," *Report No. VPI-E81.15*, Virginia Polytechnic Institute and State University, Blacksburg, VA.
7. Haftka, R. T. and Gürdal, Z., (1992). *Elements of Structural Optimization*, Kluwer Academic, Dordrecht.
8. Hanson, R. D., Aiken, I., Nims, D. K., Richter, P. J., and Bachman, R., (1993). "State-of-the-Art and State-of-the-Practice in Seismic Energy Dissipation", *ATC-17-1 Seminar on Seismic Isolation, Passive Energy Dissipation, and Active Control*, San Francisco, CA, 449-471.
9. Hanson, R., (1993). "Supplemental Damping for Improved Seismic Performance," *Earthquake Spectra*, 9(3), 319-334.
10. Housner, G. W., Bergman, L. A., Caughey, T. K., Chassiakos, A. G., Claus, R. O., Masri, S. F., Skelton, R. E., Soong, T. T., Spencer, B. F., and Yao, J. T. P.,

(1997). "Structural Control: Past, Present, and Future," *Journal of Engineering Mechanics*, 123(9), 897-971.

11. Igusa, T., Kiureghian, A. Der, and Sackman, J. L., (1984). “Modal Decomposition Method for Stationary Response of Non-classically Damped Systems,” Earthquake Engineering and Structural Dynamics, 14, 133-146.
12. Japan Building Center, (1993). "Technological Development of Earthquake-Resistant Structures," *Report of the Expert Comitee on Advanced Technology for Building Structures*, A. A. Balkema Publishers, Brookfield, VT.
13. Kanai, K., (1961). "An Empirical Formula for the Spectrum of Strong Earthquake Motions," *Bulletin Earthquake Research Institute, University of Tokyo*, 39, 85-95.
14. Lai, S.-S. P., (1982). “Statistical Characterization of Strong Ground Motions Using Power Spectral Density Functions,” *Bulletin of the Seismological Society of America*, 72(1), 259-274.
15. Makris, N. and Constantinou, M. C., (1991). "Fractional Derivative Model for Viscous Dampers," *Journal of Structural Engineering*, 117(9), 2708-2724.
16. Makris, N. and Constantinou, M. C., (1993). "Models of Viscoelasticity with Complex-Order Derivatives," *Journal of Engineering Mechanics*, 119(7), 1453-1464.
17. Makris, N., Constantinou, M. C., and Dargush, G. F., (1993a). "Analytical Model of Viscoelastic Fluid Dampers," *Journal of Structural Engineering*, 119(11), 3310-3325.
18. Makris, N., Dargush, G. F., and Constantinou, M. C., (1993b). "Dynamic Analysis of Generalized Viscoelastic Fluids," *Journal of Engineering Mechanics*, 119(8), 1663-1679.
19. Makris, N., Dargush, G. F., and Constantinou, M. C., (1995). "Dynamic Analysis of Viscoelastic Fluid Dampers," *Journal of Engineering Mechanics*, 121(10), 1114-1121.
20. Maldonado, G. O. and Singh, M. P. (1991). “An Improved Response Spectrum Method for Calculating Seismic Design Response. Part I: Non-classically

Damped Structures," *Earthquake Engineering & Structural Dynamics*, 20(7), 637-649.

21. Meirovitch, L., (1997). *Principles and Techniques of Vibrations*, Prentice-Hall, Upper Saddle River, NJ.
22. Moreschi, Luis, (2000). *Seismic Design of Energy Dissipation Systems for Optimal Structural Performance*, PhD Dissertation, Engineering Science & Mechanics, Virginia Tech.
23. Murthy, D. V. and Haftka, R. T., (1988). "Derivatives of Eigenvalues and Eigenvectors of a General Complex Matrix," *International Journal for Numerical Methods in Engineering*, 26, 293-311.
24. Rao, S. S., (1996). *Engineering Optimization*, John Wiley & Sons, New York, NY.
25. Reinhorn, A. M., Li, C., and Constantinou, M. C., (1995). "Experimental and Analytical Investigation of Seismic Retrofit of Structures with Supplemental Damping: Part 1 – Fluid Viscous Damping Devices," *Report No. NCEER 95-0001*, National Center for Earthquake Engineering Research, University of NewYork at Buffalo, Buffalo, NY.
26. Rosen, J. B., (1960). "The Gradient Projection Method for Nonlinear Programming, Part I: Linear Constraints," *SIAM Journal*, 8, 181-217.
27. Singh, M. P., (1980). "Seismic Response by SRSS for Non-proportional Damping," *Journal of Engineering Mechanics Division, ASCE*, 106, 1405-1419.
28. Singh, M. P., Chang, T. S., and Suárez, L. E., (1992). "A Response Spectrum Method for Seismic Design Evaluation of Rotating Machines," *Journal of Vibration and Acoustics*, 114, 454-460.
29. Soong, T. T. and Dargush, G. F., (1997). *Passive Energy Dissipation Systems in Structural Engineering*, John-Wiley & Sons, New York, NY.
30. Tajimi, H., (1960). "A Statistical Method of Determining the Maximum Response of a Building Structure During an Earthquake", *Proceeding of II World Conference in Earthquake Engineering*, Tokyo, 781-797.

31. Zhang, R. H. and Soong, T. T., (1989). "Seismic Response of Steel Frame Structures with Added Viscoelastic Dampers," *Earthquake Engineering and Structural Dynamics*, 18, 389-396.
32. Zhang, R. H. and Soong, T. T., (1992). "Seismic Design of Viscoelastic Dampers for Structural Applications," *Journal of Structural Engineering*, 118(5), 1375-1392.